Superelectrophilic Tetrakis(carbonyl)palladium(II)- and -platinum(II) Undecafluorodiantimonate(V), $[Pd(CO)_4][Sb_2F_{11}]_2$ and $[Pt(CO)_4][Sb_2F_{11}]_2$: Syntheses, Physical and Spectroscopic Properties, Their Crystal, Molecular, and Extended Structures, and Density Functional Calculations: An Experimental, Computational, and Comparative Study

Helge Willner,*,† Matthias Bodenbinder,‡ Raimund Bröchler,‡ Germaine Hwang,‡ Steven J. Rettig,‡ James Trotter,‡ Britta von Ahsen,† Ulrich Westphal,† Volker Jonas,§ Walter Thiel,§ and Friedhelm Aubke*,‡

Contribution from the Fachbereich 6, Anorganische Chemie, Gerhard-Mercator-Universität GH Duisburg, Lotharstrasse 1, D-47048 Duisburg, Germany, Department of Chemistry, 2036 Main Mall, The University of British Columbia, Vancouver, British Columbia, V6T 1Z1, Canada, and Max-Planck-Institut für Kohlenforschung, Kaiser-Wilhelm Platz 1, D-45470 Mülheim an der Ruhr, Germany

Received June 29, 2000

Abstract: The salts $[M(CO)_4][Sb_2F_{11}]_2$, M = Pd, Pt, are prepared by reductive carbonylation of $Pd[Pd(SO_3F)_6]$, $Pt(SO_3F)_4$ or PtF_6 in liquid SbF_5, or HF−SbF_5. The resulting moisture-sensitive, colorless solids are thermally stable up to 140 °C (M = Pd) or 200 °C (M = Pt). Their thermal decompositions are studied by differential scanning calorimetry (DSC). Single crystals of both salts are suitable for an X-ray diffraction study at 180 K. Both isostructural salts crystallize in the monoclinic space group $P2_1/c$ (No. 14). The unit cell volume of $[Pt(CO)_4][Sb_2F_{11}]_2$ is smaller than that of $[Pd(CO)_4][Sb_2F_{11}]_2$ by about 0.4%. The cations $[M(CO)_4]^{2+}$, M = Pd, Pt, are square planar with only very slight angular and out-of-plane deviations from D_{4h} symmetry. The interatomic distances and bond angles for both cations are essentially identical. The $[Sb_2F_{11}]^-$ anions in $[M(CO)_4][Sb_2F_{11}]_2$, M = Pd, Pt, are not symmetry-related, and both pairs differ in their Sb−F−Sb bridge angles and their dihedral angles. There are in each salt four to five secondary interionic C- -F contacts per CO group. Of these, two contacts per CO group are significantly shorter than the sum of the van der Waals radii by 0.58 − 0.37 Å. In addition, structural, and spectroscopic details of recently synthesized $[Rh(CO)_4][Al_2Cl_7]$ are reported. The cations $[Rh(CO)_4]^+$ and $[M(CO)_4]^{2+}$, M = Pd, Pt, are characterized by IR and Raman spectroscopy. Of the 16 vibrational modes (13 observable, 3 inactive) 10 (Pd, Pt) or 9 (Rh), respectively, are found experimentally. The vibrational assignments are supported by DFT calculations, which provide in addition to band positions also intensities of IR bands and Raman signals as well as internal force constants for the cations. ^{13}C NMR measurements complete the characterization of the square planar metal carbonyl cations. The extensive characterization of $[M(CO)_4][Sb_2F_{11}]_2$, M = Pd, Pt, reported here, allows a comparison to linear and octahedral $[M(CO)_n][Sb_2F_{11}]_2$ salts [M = Hg (n = 2); Fe, Ru, Os (n = 6)] and their derivatives, which permit a deeper understanding of M−CO bonding in the solid state for superelectrophilic cations with $[Sb_2F_{11}]^-$ or $[SbF_6]^-$ as anions.

Introduction

Square planar coordination compounds of platinum group metal ions (groups 9 and 10) with a d^8 electron configuration (Rh(I), Ir(I), Pd(II), and Pt(II)) containing π-acceptor ligands are of both historical relevancy and considerable practical importance today.

Two important milestones in the development of transition metal chemistry involve platinum(II) complexes. Zeise's salt, $K[PtCl_3(\pi\text{-}C_2H_4)]\cdot 2H_2O$, synthesized in 1827 and reported in 1831[1] is considered to be the first organo transition metal compound. Three platinum(II) carbonyl chlorides, among them *cis*-$Pt(CO)_2Cl_2$, discovered by P. Schützenberger in 1868,[2,3] are the first transition metal carbonyl complexes. Their isolation predates the synthesis of the first homoleptic metal carbonyl, $Ni(CO)_4$[4] by 22 years. The nature of the bonding in these complexes and their molecular structures however were recognized much later; for example, the molecular structure of *cis*-$Pt(CO)_2Cl_2$ was reported only a few years ago.[5]

---

* Corresponding authors. H. Willner: Telephone: 49-203-379-3309. Fax: 49-203-379-2231. E-mail: willner@uni-duisburg.de. F. Aubke: Telephone: 604-822-3817. Fax: 604-822-2847. E-mail: aubke@chem.ubc.ca.

† Gerhard-Mercator-Universität GH Duisburg.

‡ The University of British Columbia.

§ Max-Planck-Institut für Kohlenforschung.

[1] Zeise, W. C. *Annu. Rev. Phys. Chem.* **1831**, *21*, 497.

[2] Schützenberger, P. *Bull. Soc. Chim. Fr.* **1868**, *10*, 188.

[3] Schützenberger, P. *C. R. Hebd. Seances Acad. Sci.* **1870**, *10*, 134.

[4] Mond, L.; Langer, C.; Quincke, F. *J. Chem. Soc.* **1890**, 749.

[5] Bagnoli, F.; Belli Dell'Amico, D.; Calderazzo, F.; Englert, U.; Marchetti, F.; Herberich, G. E.; Pasqualetti, N.; Ramello, S. *J. Chem. Soc., Dalton Trans.* **1996**, 4317.

10.1021/ja002360s CCC: $20.00 © 2001 American Chemical Society
Published on Web 01/04/2001

There are a number of applications for square planar complexes. In homogeneous catalysis of various carbonylation-, hydrogenation-, formylation-, and hydroformylation processes, a number of square planar d^8 complexes are used as catalysts, often on an industrial scale. Two prominent examples are $RhCl(tpp)_3$, “Wilkinson’s catalyst”,[6] and *trans*-$Ir(CO)Cl(tpp)_2$, “Vaska’s compound”,[7] tpp $= P(C_6H_5)_3$. In solid-state chemistry and material sciences, stacked square planar complexes formed by tetracyanoplatinate(II) anions, $[Pt(CN)_4]^{2-}$, with various cations[8,9] or neutral halo tris(carbonyl)iridium(I) compounds, $Ir(CO)_3X$, X = Cl, Br,[8,10,11] are, after oxidative doping, one-dimensional electrical conductors.[8,9,12,13]

Even though *cis*-$Pt(CO)_2Cl_2$ is known since 1868, its square planar coordination geometry[5] is limited in metal carbonyl chemistry[14−17] largely to halo carbonyl derivatives of various metal ions from the 4d and 5d series (Rh(I), Ir(I), Pd(II), Pt(II))[14−21] with a d^8 configuration and to coordination compounds, which have a limited number of CO ligands. Of the halo carbonyl complexes, those of palladium and platinum have been widely studied,[18−24] mainly by Calderazzo and his group.[22−24] For homoleptic typical carbonyls[14−17] and highly reduced carbonylates,[25] the square planar coordination geometry is unknown. All known tetracarbonyl species are invariably tetrahedral,[14−17,25] including $Pd(CO)_4$ and $Pt(CO)_4$, which exist in inert gas matrices only.[26]

The first reported homoleptic carbonyl cations[27,28] are of the $[M(CO)_6]^+$ type, M = Mn, Tc, Re, with $[M'X_4]^-$ as counteranions, M′ = Al, Fe; X = Cl, Br, reported by E. O. Fischer et al.[29,30] and W. Hieber et al.[31−33] in the early 1960s. They form by halide abstractions from $M(CO)_5X$, M = Mn, Tc, Re; X = Cl, Br, with Lewis acids such as AlX_3 and FeX_3, X = Cl, Br, at high temperatures (∼90 °C) and high CO pressures (∼300 atm). Initial claims of the generation of $[M(CO)_6]^{2+}$ cations, M = Fe, Os,[32] by the same method have been retracted.[34] In view of the failure of these and other synthetic attempts[35] and guided by the prevailing view on metal−CO bonding, the Dewar−Chatt−Duncanson concept[36−38] with a strong emphasis on the π-back-bonding contributions to the M−CO bond,[39] metal carbonyl cations with metals in oxidation states of +2 and +3 have been viewed for a long time as incapable of existence.[40]

An alternate synthetic approach, the CO addition to metal salts of weakly coordinating anions,[41] has so far not generated any polyvalent homoleptic carbonyl cations.[42] It is also noted, that CO addition to form such molecular CO-adducts is frequently reversible at ambient conditions.[43−45]

A new synthetic methodology, the use of various superacids[46,47] as reaction media in carbonylation and solvolysis reactions, provides a viable pathway to a wide range of homoleptic metal carbonyl cations,[44,45,48] among them many superelectrophilic cations,[49] with ionic charges of +2 and +3. Superacids, which are extensively used to generate and stabilize a wide range of carbocations,[50] have found in the past only occasional use in transition metal chemistry.[15,47] The superacids employed by us are the Brønsted superacids anhydrous HF[51] and HSO_3F,[52−55] the strongest protonic acids known,[46] the Lewis superacid SbF_5,[56,57] the strongest molecular Lewis acid,[58,59] and the conjugate Brønsted−Lewis superacids, which have the highest Brønsted acidities,[46,47] $HF-SbF_5$[46,47,60,61] and HSO_3F-SbF_5[46,47,62] known as “magic acid”.[46] Isolable, thermally stable salts are frequently formed with the superacid anion $[Sb_2F_{11}]^-$,[63] which forms by self-assembly during reactions in SbF_5, $HF-SbF_5$, and surprisingly also in HSO_3F-SbF_5.[46,62]

---

(6) Young, J. F.; Osborne, J. A.; Jardine, F. H.; Wilkinson, G. *Chem. Commun.* **1965**, 131.

(7) Vaska, L.; Di Luzio, J. W. *J. Am. Chem. Soc.* **1961**, *83*, 3, 2784.

(8) Holzapfel, W.; Yersin, H.; Gliemann, G. *Z. Kristallogr.* **1981**, *57*, 47.

(9) Krogmann, K. *Angew. Chem., Int. Ed. Engl.* **1969**, *8*, 35.

(10) Hieber, W.; Lagally, H. *Z. Anorg. Allg. Chem.* **1940**, *245*, 321.

(11) Hieber, W.; Lagally, H.; Mayr, H. *Z. Anorg. Allg. Chem.* **1941**, *246*, 138.

(12) Zeller, H. R. *Adv. Solid State Phys.* **1973**, *13*, 31.

(13) Miller, J. S.; Epstein, A. J. *Prog. Inorg. Chem.* **1976**, *20*, 1.

(14) Elschenbroich, C.; Salzer, A. *Organometallics*, 2nd ed.; VCH: Weinheim, 1992.

(15) Crabtree, R. H. *The Organometallic Chemistry of the Transition Metals* ,2nd ed.; Wiley: New York, 1994; p 142.

(16) Cotton, F. A.; Wilkinson, G. *Advanced Inorganic Chemistry*, 5th ed.; Wiley: New York, 1988; p 58.

(17) Pruchnick, F. P. *Organometallic Chemistry of Transition Elements*; Plenum: New York, 1990.

(18) Tripathi, S. C.; Srivastava, S. C.; Mani, R. P.; Shrimal, A. K. *Inorg. Chim. Acta* **1976**, *17*, 257.

(19) Vergaftik, M. N.; Stromnova, T. A.; Moiseev, I. I. *Russ. J. Inorg. Chem.* **1980**, *25*, 127.

(20) Stromnova, T. A.; Moiseev, I. I. *Russ. Chem. Rev.* **1998**, *67*, 485.

(21) Roundhill, M. *Comprehensive Coordination Chemistry*; Pergamon Press: Oxford, 1987; Vol. 5, p 351.

(22) Calderazzo, F. *J. Organomet. Chem.* **1990**, *400*, 303.

(23) Calderazzo, F. *Pure Appl. Chem.* **1978**, *50*, 49.

(24) Calderazzo, F.; Belli Dell’Amico, D. *Pure Appl. Chem.* **1986**, *58*, 561.

(25) Ellis, J. E. *Adv. Organomet. Chem.* **1990**, *31*, 1.

(26) Moskovits, M.; Ozin, G. A. *Cryochemistry*; Wiley: New York, 1976, and references therein.

(27) Abel, E. W.; Tyfield, S. P. *Adv. Organomet. Chem.* **1970**, *8*, 117.

(28) Beck, W.; Sünkel, K. *Chem. Rev.* **1988**, *88*, 1405.

(29) Fischer, E. O.; Fichtel, K.; Öfele, K. *Chem. Ber.* **1961**, *94*, 1200.

(30) Fischer, E. O.; Fichtel, K.; Öfele, K. *Chem. Ber.* **1962**, *95*, 249.

(31) Hieber, W.; Lux, F.; Herget, C. *Z. Naturforsch., B: Chem. Sci.* **1965**, *20*, 1159.

(32) Hieber, W.; Kruck, T. *Angew. Chem.* **1961**, *73*, 580.

(33) Hieber, W.; Kruck, T. *Z. Naturforsch., B: Chem. Sci.* **1961**, *16*, 709.

(34) Hieber, W.; Frey, V.; John, P. *Chem. Ber.* **1967**, *100*, 1961.

(35) Sternberg, H. W.; Friedel, A. R.; Shufler, S. L.; Wender, I. *J. Am. Chem. Soc.* **1955**, *77*, 2675.

(36) Dewar, J. S. *Bull. Soc. Chim. Fr.* **1951**, *18*, C71.

(37) Chatt, J.; Duncanson, L. A. *J. Chem. Soc.* **1953**, 2939.

(38) Chatt, J.; Wilkins, R. G. *J. Chem. Soc.* **1952**, 2622.

(39) Pearson, R. G. *Inorg. Chem.* **1984**, *23*, 4675.

(40) Hieber, W. *Adv. Organomet. Chem.* **1970**, *8*, 1.

(41) Strauss, S. H. *Chem. Rev.* **1993**, *93*, 927.

(42) Lupinetti, A. J.; Frenking, G.; Strauss, S. H. *Prog. Inorg. Chem.*, in press.

(43) Strauss, S. H. *Chemtracts: Inorg. Chem.* **1997**, *10*, 777.

(44) Aubke, F.; Wang, C. *Coord. Chem. Rev.* **1994**, *137*, 483.

(45) Weber, L. *Angew. Chem., Int. Ed. Engl.* **1994**, *33*, 1077.

(46) Olah, G. A.; Prakash, G. K. S.; Sommer, J. *Superacids*; Wiley: New York, 1985.

(47) O’Donnell, T. A. *Superacids and Acidic Melts as Inorganic Reaction Media*; VCH: Weinheim, Germany, 1993.

(48) Willner, H.; Aubke, F. *Angew. Chem., Int. Ed. Engl.* **1997**, *36*, 2402.

(49) Olah, G. A. *Angew. Chem., Int. Ed. Engl.* **1993**, *32*, 767.

(50) Olah, G. A.; von Schleyer, P. *Carbonium Ions*; Wiley-Interscience: New York, 1968, 1970, 1972, 1973, 1976; Vol. I−V.

(51) Hyman, H. H.; Katz, J. J. In *Non-Aquous Solvent Systems*; Waddington, T. C., Ed.; Academic Press: New York, 1965; p 47.

(52) Gillespie, R. J. *Acc. Chem. Res.* **1968**, *1*, 202.

(53) Thompson, R. C. In *Inorganic Sulphur Chemistry*; Nickless, G., Ed.; Elsevier: Amsterdam, 1968; p 587.

(54) Jache, A. W. *Adv. Inorg. Radiochem.* **1974**, *16*, 177.

(55) Barr, J.; Gillespie, R. J.; Thompson, R. C. *Inorg. Chem.* **1964**, *3*, 1149.

(56) Kemmit, R. D.; Sharp, D. W. A. *Advances in Fluorine Chemistry*; Butterworth: London, 1965; Vol. 4, p 210.

(57) Wang, C.; Hwang, G.; Siu, S. C.; Bley, B.; Bodenbinder, M.; Bach, C.; Willner, H.; Aubke, F. *Eur. J. Solid State Inorg. Chem.* **1996**, *74*, 1952.

(58) Fabré, P. L.; Devynk, J.; Tremillon, B. *Chem. Rev.* **1982**, *82*, 591.

(59) Christe, K. O.; Dixon, D. A.; McLemore, D.; Wilson, W. W.; Sheehy, J. A.; Boatz, J. A. *J. Fluorine Chem.* **2000**, *101*, 151.

(60) Hyman, H. H.; Quaterman, L.; Kilpatrick, P. M.; Katz, J. J. *J. Phys. Chem.* **1961**, *65*, 123.

(61) Gillespie, R. J.; Moss, K. C. *J. Chem. Soc. A* **1966**, 1170.

(62) Zhang, D.; Heubes, M.; Haegele, G.; Aubke, F. *Can. J. Chem.* **1999**, *77*, 1869.

(63) Zhang, D.; Rettig, S. J.; Trotter, J.; Aubke, F. *Inorg. Chem.* **1996**, *35*, 6113.

Following the generation of linear $[Au(CO)_2]^+_{(solv)}$ in HSO_3F solution[64] by reductive carbonylation of $Au(SO_3F)_3$[65,66] in 1990 and the subsequent conversion of the intermediate $Au(CO)SO_3F$[64] into the thermally stable salt $[Au(CO)_2][Sb_2F_{11}]$ by solvolytic carbonylation in SbF_5,[67] the same synthetic approach has been applied to the reductive carbonylation of $Pd[Pd(SO_3F)_6]$[68,69] and $Pt(SO_3F)_4$,[70] respectively. In complete analogy to the gold(I) carbonyl system, the solvated cations $[M(CO)_4]^{2+}_{(solv)}$, M = Pd, Pt, form initially in HSO_3F, but the fluorosulfates *cis*-$M(CO)_2(SO_3F)_2$, M = Pd, Pt, are eventually isolated.[71] The molecular structures of *cis*-$M(CO)_2(SO_3F)_2$, M = Pd,[72] Pt,[73] are known. The $[Pt(CO)_4]^{2+}$ cation is isolated from HSO_3F in the initial stages of the reductive carbonylation of $Pt(SO_3F)_4$ as $[Pt(CO)_4][Pt(SO_3F)_6]$.[74] The self-ionization ion $[Pt(SO_3F)_6]^{2-}$ of the diprotic conjugate superacid $HSO_3F-Pt(SO_3F)_4$,[70] is structurally characterized as cesium salt.[63] In liquid SbF_5 in a CO atmosphere both *cis*-$M(CO)_2(SO_3F)_2$, M = Pd, Pt, are easily converted to $[M(CO)_4][Sb_2F_{11}]_2$, M = Pd, Pt. The syntheses and the vibrational spectra in the CO-stretching region are reported in a preliminary communication.[75] The square planar coordination geometry of the cations is easily deduced from their vibrational spectra.

Subsequently a number of additional, highly unusual superelectrophilic metal carbonyl cations are obtained as $[Sb_2F_{11}]^-$ salts from SbF_5 or $HF-SbF_5$ as reaction media. They include linear $[Hg(CO)_2]^{2+}$,[76,77] the first, and so far only, thermally stable homoleptic carbonyl cation formed by a post-transition metal,[48] $[Ir(CO)_6]^{3+}$,[78] the first tripositive metal carbonyl cation, $[Fe(CO)_6]^{2+}$, the first dipositive cation formed by a 3d metal,[79,80] octahedral $[M(CO)_6]^{2+}$, M = Ru, Os,[81,82] the monochloro pentacarbonyl cations $[M(CO)_5Cl]^{2+}$, M = Rh, Ir,[78,83] and the group 6 hexafluoro antimonato(V) cations $[W(CO)_6(FSbF_5)]^+$ [84] and cyclic $[\{Mo(CO)_4\}_2(\mu\text{-}F_2SbF_4)_3]^+$ [85] as part of a polymeric chain.

All of these, with the exception of $[Ir(CO)_6]^{3+}$,[78] are structurally characterized by single-crystal X-ray diffraction with $[Sb_2F_{11}]^-$ as counteranion.[77,78,80,82−85] In all instances significant interionic C- -F contacts are observed, resulting in extended molecular structures. The salts $[M(CO)_6][Sb_2F_{11}]_2$, M = Fe, Ru, Os, are readily converted to their related $[SbF_6]^-$-salts, whose molecular structures are obtained as well.[80,82]

The cation $[Pt(CO)_4]^{2+}$ is found with three different counteranions, $[Sb_2F_{11}]^-$,[75] $[Pt(SO_3F)_6]^{2-}$[74] and $[PtF_6]^{2-}$,[86] while $[Pd(CO)_4][Sb_2F_{11}]_2$[75] and the precursor *cis*-$Pd(CO)_2(SO_3F)_2$[71,72] appear to be the only true cationic polycarbonyl derivatives of palladium(II),[20] with the possible exception of thermally unstable $Pd(CO)_2R_2$, R = C_6F_5, C_6Cl_5.[87] An early claim of the synthesis of *cis*-$Pd(CO)_2Cl_2$[88] has been repudiated,[89] and the reported crystal structure and spectroscopic properties of "$[Pd(\mu\text{-}Cl)(CO)_2]_2$"[90] are evidently identical in all respects to those of well-known $[Rh(\mu\text{-}Cl)(CO)_2]_2$.[91,92]

The objectives of this study are: (i) to summarize and to evaluate a number of alternative synthetic routes to both $[Pd(CO)_4]^{2+}$ [93] and $[Pt(CO)_4]^{2+}$ salts,[86,93] (ii) to investigate the thermal behavior of $[M(CO)_4][Sb_2F_{11}]_2$, M = Pd, Pt, in detail, (iii) to report the crystal, molecular and extended structures of $[M(CO)_4][Sb_2F_{11}]_2$, M = Pd, Pt. Square planar homoleptic metal carbonyls are, as discussed, exceedingly rare.[14−17,25] Only very recently the structural characterization of square planar $[Rh(CO)_4]^+$ has been achieved with either $[1\text{-Et-CB}_{11}F_{11}]^-$ [94] or $[Al_2Cl_7]^-$ [95] as counteranion, (iv) to analyze the complete vibrational spectra of the cations $[M(CO)_4]^{2+}$, M = Pd, Pt, and $[Rh(CO)_4]^+$ (D_{4h}). Such an analysis has been reported so far only for the homoleptic carbonyl cations $[Au(CO)_2]^+$ (D_{4h})[67] and $[Fe(CO)_6]^{2+}$ (O_h)[80], (v) to perform density functional calculations of $[M(CO)_4]^{2+}$, M = Pd, Pt, which are extended to include in addition to the known cation $[Rh(CO)_4]^+$ [94,95] the probable cations $[Co(CO)_4]^+$ and $[Ir(CO)_4]^+$, as well as the hypothetical cations $[Ni(CO)_4]^{2+}$, $[Au(CO)_4]^{3+}$, and $[Hg(CO)_4]^{4+}$. The calculations address the molecular structures, vibrational assignments and atomic charge distribution for square planar $[M(CO)_4]^{n+}$ cations. Thus far, theoretical calculations of existing homoleptic carbonyls have been limited to octahedral species[83,96−100] and linear d^{10} ions.[101−104]

Both $[Pt(CO)_4][Sb_2F_{11}]_2$ and $[Pd(CO)_4][Sb_2F_{11}]_2$ and other metal carbonyl cations are not strictly of academic interest only.

---

(64) Willner, H.; Aubke, F. *Inorg. Chem.* **1990**, *29*, 2195.

(65) Lee, K. C.; Aubke, F. *Inorg. Chem.* **1979**, *18*, 389.

(66) Lee, K. C.; Aubke, F. *Inorg. Chem.* **1980**, *19*, 119.

(67) Willner, H.; Schaebs, J.; Hwang, G.; Mistry, F.; Jones, R.; Trotter, J.; Aubke, F. *J. Am. Chem. Soc.* **1992**, *114*, 8972.

(68) Lee, K. C.; Aubke, F. *Can. J. Chem.* **1977**, *55*, 2473.

(69) Lee, K. C.; Aubke, F. *Can. J. Chem.* **1979**, *57*, 2058.

(70) Lee, K. C.; Aubke, F. *Inorg. Chem.* **1984**, *23*, 2124.

(71) Hwang, G.; Wang, C.; Bodenbinder, M.; Willner, H.; Aubke, F. *J. Fluorine Chem.* **1994**, *66*, 159.

(72) Wang, C.; Willner, H.; Bodenbinder, M.; Batchelor, J.; Einstein, F. W. B.; Aubke, F. *Inorg. Chem.* **1994**, *33*, 3521.

(73) von Ahsen, B.; Wartchow, R.; Willner, H.; Jonas, V.; Aubke, F. *Inorg. Chem.* **2000**, *39*, 4424.

(74) Hwang, G.; Bodenbinder, M.; Willner, H.; Aubke, F. *Inorg. Chem.* **1993**, *32*, 4667.

(75) Hwang, G.; Wang, C.; Aubke, F.; Willner, H.; Bodenbinder, M. *Can. J. Chem.* **1993**, *71*, 1532.

(76) Willner, H.; Bodenbinder, M.; Wang, C.; Aubke, F. *J. Chem. Soc., Chem. Commun.* **1994**, 1189.

(77) Bodenbinder, M.; Balzer-Jöllenbeck, G.; Willner, H.; Batchelor, R. J.; Einstein, F. W. B.; Wang, C.; Aubke, F. *Inorg. Chem.* **1996**, *35*, 82.

(78) Bach, C.; Willner, H.; Wang, C.; Rettig, S. J.; Trotter, J.; Aubke, F. *Angew. Chem., Int. Ed. Engl.* **1996**, *35*, 1974.

(79) Bley, B.; Willner, H.; Aubke, F. *Inorg. Chem.* **1997**, *36*, 158.

(80) Bernhardt, E.; Bley, B.; Wartchow, R.; Willner, H.; Bill, E.; Kuhn, P.; Sham, I. H. T.; Bodenbinder, M.; Bröchler, R.; Aubke, F. *J. Am. Chem. Soc.* **1999**, *121*, 7188.

(81) Wang, C.; Bley, B.; Balzer-Jöllenbeck, G.; Lewis, A. R.; Sui, S. C.; Willner, H.; Aubke, F. *J. Chem. Soc., Chem. Commun.* **1995**, 2071.

(82) Bernhardt, E.; Bach, C.; Wartchow, R.; Willner, H.; Aubke, F. *Inorg. Chem.* Manuscript to be submitted.

(83) Willner, H.; Bach, C.; Wartchow, R.; Wang, C.; Rettig, S. J.; Trotter, J.; Jonas, V.; Thiel, W.; Aubke, F. *Inorg. Chem.* **2000**, *39*, 1933.

(84) Bröchler, R.; Sham, I. H. T.; Bodenbinder, M.; Schmitz, V.; Rettig, S. J.; Trotter, J.; Willner, H.; Aubke, F. *Inorg. Chem.* **2000**, *39*, 2172.

(85) Bröchler, R.; Freidank, D.; Bodenbinder, M.; Sham, I. H. T.; Willner, H.; Rettig, S. J.; Trotter, J.; Aubke, F. *Inorg. Chem.* **1999**, *38*, 3684.

(86) von Ahsen, B.; Bach, C.; Pernice, H.; Willner, H.; Aubke, F. *J. Fluorine Chem.* **2000**, *102*, 243.

(87) Uson, R.; Fornies, J.; Tomas, M.; Menjon, B. *Organometallics* **1985**, *4*, 1912.

(88) Fink, E. *C. R. Hebd. Seances Acad. Sci.* **1898**, *126*, 646.

(89) Manchot, W.; König, J. *Chem. Ber.* **1926**, *59*, 883.

(90) Soriano-Garcia, M.; Rosa, N.; Gomez-Lara, J.; Toscana, R. A. *Acta Crystallogr., Sect. C* **1987**, *43*, 1679.

(91) Dahl, L. F.; Martell, C.; Wampler, D. L. *J. Am. Chem. Soc.* **1961**, *83*, 1761.

(92) Yang, A. C.; Garland, C. W. *J. Phys. Chem.* **1957**, *61*, 1504.

(93) Wang, C.; Siu, S. C.; Hwang, G.; Bach, C.; Bley, B.; Bodenbinder, M.; Willner, H.; Aubke, F. *Can. J. Chem.* **1996**, *74*, 1952.

(94) Lupinetti, A. J.; Havighurst, M. D.; Miller, S. M.; Anderson, O. P.; Strauss, S. H. *J. Am. Chem. Soc.* **1999**, *121*, 11920.

(95) von Ahsen, B.; Bach, C.; Köckerling, M.; Willner, H.; Aubke, F. Manuscript in preparation.

(96) Ehlers, A. W.; Ruiz-Morales, Y.; Baerends, E. J.; Ziegler, T. *Inorg. Chem.* **1997**, *36*, 5031.

(97) Szillagy, R. K.; Frenking, G. *Organometallics* **1997**, *16*, 4807.

(98) Jonas, V.; Thiel, W. *Organometallics* **1998**, *17*, 353.

(99) Frenking, G.; Fröhlich, N. *Chem. Rev.* **2000**, *100*, 717.

(100) Diefenbach, A.; Bickelhaupt, F. M.; Frenking, G. *J. Am. Chem. Soc.* **2000**, *122*, 6449.

(101) Veldkamp, A.; Frenking, G. *Organometallics* **1993**, *12*, 82.

(102) Lynn, M. A.; Bursten, B. E. *Inorg. Chim. Acta* **1995**, *229*, 437.

(103) Lupinetti, A. J.; Jonas, V.; Thiel, W.; Strauss, S. H.; Frenking, G. *Chem. Eur. J.* **1999**, *5*, 2573.

(104) Jonas, V.; Thiel, W. *J. Chem. Soc., Dalton Trans.* **1999**, 3783.

A recent report on the use of $[Pt(CO)_4][Sb_2F_{11}]_2$ as polymerization catalyst[105] and the use of various cationic carbonyl complexes in the carbonylation of olefins[106−109] suggest beginning practical applications of these materials. The existence of derivatives such as dinuclear $[\{Pt(CO)_3\}_2]^{2+}$ in H_2SO_4[110] and of cations such as $[cyclo\text{-}C_2H_4\{P(R_F)_2\}_2Pt(CO)_2]^{2+}$, $R_F = C_2F_5$,[111] which are generated in superacids, points to the emergence of a viable new chemistry of cationic platinum carbonyl derivatives.

Experimental Section

Apparatus. Volatile materials were manipulated in Monel or Pyrex vacuum-lines of known volume. The monel lines were fitted with Whitey valves RS4-316 and Swagelok fittings, while the Pyrex vacuum line was fitted with Teflon stem valves. Both lines were equipped with capacitance pressure gauges (type 280 E Setra Instruments, Acton, MA). For reactions in SbF_5 or HSO_3F Pyrex reactors of ∼50 mL volume were used, fitted with Kontes valves and Teflon-coated magnetic stirring bars. Reactions in anhydrous HF or in HF−SbF_5 as well as recrystallizations were carried out in Kel-F reaction vials of about 30 mL volume, fitted with a Monel top, equipped with a stainless steel Whitey valve RS4-316. A drawing of the reactor is included in the Supporting Information as Figure S1. Solid materials were manipulated in a Vacuum Atmosphere Corporation Dry-Lab model DI 001-SG dry box filled with nitrogen and fitted with a HE 493 Dry Train.

Chemicals and Synthetic Procedures. Platinum and palladium powder (both 99.9% pure) were obtained as a gift from the Degussa-Hüls Company. Fluorosulfuric acid tech. grade (Orange County Chemicals) was purified by double distillation at room temperature as described previously.[55] Antimony(V) fluoride (Atochem North America, formerly Ozark-Mahoning) was purified by atmospheric pressure distillation, followed by a vacuum distillation. To remove moisture as $[H_3O][Sb_2F_{11}]$,[63] a small amount of SbF_5 was added to anhydrous HF (Air Products), and the mixture was stored in a Kel-F vial. Bis(fluorosulfuryl)peroxide, $S_2O_6F_2$ was synthesized by catalytic (AgF_2) fluorination of SO_3[112] (Dupont) with elemental fluorine (Air Products) as described.[112,113] The starting materials and intermediates $Pt(SO_3F)_4$,[70] $Pd[Pd(SO_3F)_6]$,[68,69] and $cis\text{-}M(CO)_2(SO_3F)_2$,[71] M = Pd, Pt, were all obtained according to published methods. $[Pt(CO)_4][Sb_2F_{11}]_2$ was prepared from $cis\text{-}Pt(CO)_2(SO_3F)_2$ by carbonylation in liquid SbF_5 as described.[75] $[Pd(CO)_4][Sb_2F_{11}]_2$ was obtained by the reductive carbonylation of $Pd[Pd(SO_3F)_6]$ in HF−SbF_5. Carbon monoxide (CP grade, stated purity 99.5%) was obtained from Medigas Corp. and purified by passing the gas through a trap cooled to −196 °C. ^{13}CO (99% enriched) was obtained from IC Chemicals.

Warning: Of the reagents used in this study HF, HSO_3F, F_2, CO, SO_3, SbF_5, and $S_2O_6F_2$ are either highly corrosive, strongly oxidizing or toxic. Vacuum lines, used for the handling of these reagents, are contained inside of well ventilated, fume hoods. Safety equipment should be worn and available safety information sheets should be consulted together with the original literature cited here, when attempting the reactions described.

Instrumentation. (a) Vibrational Spectroscopy. Infrared spectra were recorded at room temperature on an IFS-66v FT spectrometer (Bruker, Karlsruhe, Germany). Two different detectors together with a Ge/KBr or a 6 μm Mylar beam splitter operating in the region 5000−400 or 550−80 cm^{-1}, respectively, were used. One hundred and twenty eight scans were co-added for each spectrum, using an apodized resolution of 2 or 4 cm^{-1}. The samples were crushed between CaF_2, AgBr (Korth, Kiel, Germany), or polyethylene (Cadillac, Hannover, Germany) disks inside the drybox. **Raman spectra** were recorded at room temperature with a Bruker RFS 100/S FT Raman spectrometer using the 1064 nm exciting line (∼500 mW) of a Nd:YAG laser (Adlas, DPY 301, Lübeck, Germany). Crystalline samples were contained in large melting point capillaries (2 mm od.) for recording spectra in the region 5000−80 cm^{-1} with a spectral resolution of 2 cm^{-1}.

Table 1. Crystallographic Data for $[M(CO)_4][Sb_2F_{11}]_2$, M = Pd, Pt[a]

compound	$[Pd(CO)_4][Sb_2F_{11}]_2$	$[Pt(CO)_4][Sb_2F_{11}]_2$
empirical formula	$C_4F_{22}O_4PdSb_4$	$C_4F_{22}O_4PtSb_4$
formular weight	1123.41	1212.10
crystal system	monoclinic	monoclinic
space group	No. 14, $P2_1/c$	No. 14, $P2_1/c$
a [Å]	12.583(2)	12.757(2)
b [Å]	9.8172(9)	9.726(2)
c [Å]	17.9895(7)	17.8576(7)
β [deg]	103.1183(10)	103.3576(7)
V [Å^3]	2164.2(4)	2155.7(5)
Z	4	4
ρ_{calc} [g/cm^3]	3.448	3.734
T [°C]	−93(1)	−93(1)
radiation	Mo Kα	Mo Kα
λ [Å]	0.71069	0.71069
μ [cm^{-1}]	59.35	115.80
R (F)	0.025	0.025
R_w (F^2)	0.047	0.048

[a] $R = \Sigma||F_o| - |F_c||/\Sigma|F_o|$ $(I \geq 3\sigma(I))$, $R_w = (\Sigma w(|F_o^2| - |F_c^2|)^2/\Sigma w|F_o^2|^2)^{1/2}$ (all data)

(b) NMR Spectroscopy. ^{13}C NMR spectra were obtained on a Bruker MSL-200 FT spectrometer, operating at 50.322 MHz. Solid-state ^{13}NMR spectra (MAS) were recorded using a broad band probe MAS DLK 39−82 MHz. Samples were contained in ZrO_2 crucibles (7 mm in diameter) fitted with a Kel-F insert and lid. The rotational frequency was 5 kHz for $[M(CO)_4][Sb_2F_{11}]_2$, M = Pd, Pt. Adamantane (28.8 and 37.9 ppm) was used as a standard, and measured chemical shifts were converted to the TMS scale.

(c) X-ray Diffraction. All measurements were made at 180 ± 1 K on a Rigaku/ADSC-CCD area detector diffractometer using graphite monochromated Mo Kα radiation. X-ray crystallographic analyses of $[M(CO)_4][Sb_2F_{11}]_2$, M = Pd, Pt: Crystallographic data appear in Table 1. The final unit-cell parameters were based on 11 367 (Pd) and 11 597 (Pt) reflections respectively with $2\Theta = 4-60°$. The data were processed[114,115] and corrected for Lorentz and polarization effects and absorption (semiempirical multiscan, based on a three-dimensional analysis of symmetry-equivalent data). The structures were solved by direct methods. All atoms were refined with anisotropic thermal parameters. No secondary extinction corrections were necessary. Neutral atom scattering factors and anomalous dispersion corrections were taken from the International Tables for X-ray Crystallography.[116,117]

(d) Differential Scanning Calorimetry (DSC). Thermo-analytical measurements were made with a Netzsch DSC 204 instrument. Temperature and sensitivity calibrations in the temperature range of 20−500 °C were carried out with naphthalene, benzoic acid, KNO_3, $AgNO_3$, $LiNO_3$, and CsCl. The heating rate employed was 10 K min^{-1}, and the furnace was flushed with dry nitrogen. For the evaluation, the software Netzsch Proteus 4.0 was employed.

The samples were contained in sealed stainless steel crucibles, which were coated on the inside with gold or rhodium (courtesy of Degussa-Hüls), of an approximate mass of 1.3 g and a volume of 100 μL, which

---

(105) Weber, L.; Barlmeyer, M.; Quasdorff, J. M.; Sievers, H. L.; Stammler, H.-G.; Neumann, B. *Organometallics* **1999**, *18*, 2497.

(106) Xu, Q.; Souma, Y.; Umezawa, J.; Tanaka, M.; Nakatani, H. *J. Org. Chem.* **1999**, *64*, 6306.

(107) Xu, Q.; Souma, Y. *Top. Catal.* **1998**, *6*, 17.

(108) Xu, Q.; Imamura, Y.; Fujiwara, M.; Souma, Y. *J. Org. Chem.* **1997**, *62*, 1594.

(109) Xu, Q.; Nakatani, H.; Souma, Y. *J. Org. Chem.* **2000**, *65*, 1540.

(110) Xu, Q.; Heaton, B. T.; Jacob, C.; Mogi, K.; Ichihashi, Y.; Souma, Y.; Kanamori, K.; Eguchi, T. *J. Am. Chem. Soc.* **2000**, *122*, 6862.

(111) Houlis, J. F.; Roddick, D. M. *J. Am. Chem. Soc.* **1998**, *120*, 11020.

(112) Dudley, F. B.; Cady, G. H. *J. Am. Chem. Soc.* **1957**, *79*, 513.

(113) Zhang, D.; Wang, C.; Mistry, F.; Powell, B.; Aubke, F. *J. Fluorine Chem.* **1996**, *76*, 83.

(114) *teXsan: Crystal Structure Analysis Package 1.8*; Molecular Structure Corp.: The Woodlands, TX; 1996.

(115) *d*TREK: Area Detector Software*; Molecular Structure Corp.: The Woodlands, TX; 1998.

(116) *International Tables for X-ray Crystallography*; Kynoch Press (present distributor Kluwer Academic Publishers: Boston, MA): Birmingham, UK, 1974; Vol. IV, p 99.

(117) *International Tables for Crystallography*; Kluwer Academic Publishers: Boston, MA, 1992; Vol. C, p 200.

stood up to a pressure of 100 bar. In an inert atmosphere about 25−40 mg of the solid sample was weighed. Samples were studied in the temperature range of 25−300 °C. After completion of each run, the crucible lid was punctured in vacuo, the gaseous products as well as the solid residues were studied by IR spectroscopy.

Synthetic Reactions and Crystal Growth. General Comments. The routes to $[M(CO)_4][Sb_2F_{11}]_2$, M = Pd, Pt, involved the reductive carbonylation of $Pd[Pd(SO_3F)_6]$[68,69] in HF−SbF_5[93] or of $Pt(SO_3F)_4$[70] in HSO_3F, followed by the isolation of *cis*-$Pt(CO)_2(SO_3F)_2$[71] and the subsequent solvolytic carbonylation to $[Pt(CO)_4][Sb_2F_{11}]_2$.

(a) $[Pt(CO)_4][Sb_2F_{11}]_2$. For crystal growth approximately 0.5 g of $[Pt(CO)_4][Sb_2F_{11}]_2$ were dissolved in a mixture of ∼10% of SbF_5 and ∼90% (by volume) of anhydrous HF. CO was added to give a total pressure of ∼1.5 atm. A small amount of the substance remained undissolved. The suspension was heated briefly (about 30 min) to 60 °C while stirring and allowed to cool to room temperature without stirring. The solvent was then removed slowly in vacuo over a period of 24 h. The mixture had darkened due to the formation of traces of platinum. From the dry, gray powder small crystals of $[Pt(CO)_4][Sb_2F_{11}]_2$ were picked inside a drybox under a polarizing microscope and fitted into Lindemann glass capillaries.

(b) $[Pd(CO)_4][Sb_2F_{11}]_2$. The salt was obtained by the reductive carbonylation of ∼0.2 g of $Pd[Pd(SO_3F)_6]$ in 10 mL of HF−SbF_5 (1:1 by volume), adopted from a published procedure.[93] The mixture was heated at 60 °C and ∼1.5 atm of CO for 24 h and was then allowed to cool to room temperature. The solid product mixture contained a number of small crystals which were picked under a polarizing microscope and fitted into Lindemann glass capillaries inside a drybox.

The ^{13}C-isotopomers $[M(^{13}CO)_4][Sb_2F_{11}]_2$, M = Pd, Pt, were obtained by using ^{13}CO throughout the reductive carbonylations of $Pt(SO_3F)_4$ or $Pd[Pd(SO_3F)_6]$ in SbF_5.

Theoretical Methods

Gradient-corrected density functional calculations were carried out by using the Gaussian94[118] and Gaussian98[119] program systems. Gradient corrections for exchange and for correlation were taken from the work of Becke[120] and Perdew,[121] respectively (usually abbreviated as BP or BP86). Two basis sets were employed, labeled ECP1 and ECP2. Both used a quasi relativistic effective core potential at the transition metal together with the corresponding (8s,7p,5d)/[6s,5p,3d] valence basis set.[122,123] For carbon and oxygen, ECP1 employed the 6-31G(d) basis,[124,125] whereas ECP2 used a Dunning (10s,6p)/[5s,3p] triple-ζ basis supplemented by two sets of d polarization functions.[126,127] Spherical d-functions were applied throughout. Using analytic energy gradients, the molecular geometries were optimized within the constraint of D_{4h} point group symmetry. Second derivatives were obtained by numerical differentiation of the analytic energy gradients with Gaussian94 or analytically with Gaussian98, which also provided Raman intensities at the BP86/ECP2 level. The present computational approach was the same as in previous studies.[98−100,128−130]

Results and Discussion

Synthetic Aspects. Both $[Pd(CO)_4][Sb_2F_{11}]_2$ and $[Pt(CO_4][Sb_2F_{11}]_2$ together with $[Pt(CO)_4][Pt(SO_3F)_6]$ are the first of a growing list of superelectrophilic[49] metal carbonyl cations, and the only ones of these with a square planar coordination geometry. The superacid anion $[Pt(SO_3F)_6]^{2-}$ ranks just below $[Sb_2F_{11}]^-$ and $[SbF_6]^-$ as a very weak nucleophile in an order based on ^{119}Sn Mössbauer spectroscopy of various dimethyl tin(IV) salts.[131]

The previously reported syntheses of $[M(CO)_4][Sb_2F_{11}]_2$, M = Pd, Pt,[75] involve the solvolytic carbonylation of the *cis*-$M(CO)_2(SO_3F)_2$, M = Pd, Pt,[71] which in turn are obtained by the reductive carbonylation of $Pd[Pd(SO_3F)_6]$[68,69] or $Pt(SO_3F)_4$[70] in HSO_3F. The two precursors[68−70] are obtained by the oxidation of Pd or Pt metal powder, respectively, with $S_2O_6F_2$[112,113] in HSO_3F[52−56] as described.[68−70] There are a number of simpler alternative routes to $[Pt(CO)_4][Sb_2F_{11}]_2$ and to a lesser extent to $[Pd(CO)_4][Sb_2F_{11}]_2$, which are reviewed recently.[73]

In liquid SbF_5, the reductive carbonylations of both $Pd[Pd(SO_3F)_6]$[68,69] and $Pt(SO_3F)_4$[70] lead directly to $[M(CO)_4][Sb_2F_{11}]_2$, M = Pd, Pt.[93] We have shown, in the course of this study, that in HF−SbF_5 crystalline $[Pd(CO)_4][Sb_2F_{11}]_2$ is directly obtained by this route from the mixed valency palladium fluorosulfate.

The most elegant synthesis of $[Pt(CO)_4][Sb_2F_{11}]_2$ is the reductive carbonylation of PtF_6 in liquid SbF_5[86] according to:

$$PtF_6 + 6\,CO + 4\,SbF_5 \xrightarrow[SbF_{5(l)},\ 1\ atm\ CO]{25-50\ °C,\ 2\ h} [Pt(CO)_4][Sb_2F_{11}]_2 + 2\,COF_2 \quad (1)$$

This approach, which produces only a single, volatile byproduct, is efficient and fast. However the synthesis of PtF_6 is not trivial.[86,132−134] Interestingly, the reductive carbonylation of PtF_6 in pure anhydrous HF produces $[Pt(CO)_4][PtF_6]$, which is the first example of a Pt(II) carbonyl fluoride after recent unsuccessful attempts to synthesize *cis*-$Pt(CO)_2F_2$.[73] As is generally observed, late transition metal carbonyl fluorides are rather uncommon.[135,136] Attempts to convert $[M(CO)_4][Sb_2F_{11}]_2$, M = Pd, Pt, into the $[SbF_6]^-$ salts by repeated washing with anhydrous HF in order to produce $[M(CO)_4][SbF_6]_2$, M = Pd, Pt, are unsuccessful.

All synthetic routes to $[M(CO)_4]^{2+}$, M = Pd, Pt, salts involve $Pd[Pd(SO_3F)_6]$,[68,69] $Pt(SO_3F)_4$[70] or PtF_6[86,132,133] as starting materials, which are not commercially available. Their synthesis

---

(118) Frisch, M. J.; Trucks, G. W.; Schlegel, H. B.; Gill, P. M. W.; Johnson, B. G.; Robb, M. A.; Cheeseman, J. R.; Keith, T.; Petersson, G. A.; Montgomery, J. A., Jr.; Raghavachari, K.; Al-Laham, M. A.; Zakrzewski, V. G.; Ortiz, J. V.; Foresman, J. B.; Cioslowski, J.; Stefanov, B. B.; Nanayakkara, A.; Challacombe, M.; Peng, C. Y.; Ayala, P. Y.; Chen, W.; Wong, M. W.; Andres, J. L.; Replogle, E. S.; Gomperts, R.; Martin, R. L.; Fox, D. J.; Binkley, J. S.; Defrees, D. J.; Baker, J.; Stewart, J. P.; Head-Gordon, M.; Gonzalez, C.; Pople, J. A. *Gaussian 94,* Revision D.4; Gaussian, Inc.: Pittsburgh, PA, 1995.

(119) Frisch, M. J.; Trucks, G. W.; Schlegel, H. B.; Scuseria, G. E.; Robb, M. A.; Cheeseman, J. R.; Zakrzewski, V. G.; Montgomery, J. A., Jr.; Stratmann, R. E.; Burant, J. C.; Dapprich, S.; Millam, J. M.; Daniels, A. D.; Kudin, K. N.; Strain, M. C.; Farkas, O.; Tomasi, J.; Barone, V.; Cossi, M.; Cammi, R.; Mennucci, B.; Pomelli, C.; Adamo, C.; Clifford, S.; Ochterski, J.; Petersson, G. A.; Ayala, P. Y.; Cui, Q.; Morokuma, K.; Malick, D. K.; Rabuck, A. D.; Raghavachari, K.; Foresman, J. B.; Cioslowski, J.; Ortiz, J. V.; Stefanov, B. B.; Liu, G.; Liashenko, A.; Piskorz, P.; Komaromi, I.; Gomperts, R.; Martin, R. L.; Fox, D. J.; Keith, T.; Al-Laham, M. A.; Peng, C. Y.; Nanayakkara, A.; Gonzalez, C.; Challacombe, M.; Gill, P. M. W.; Johnson, B.; Chen, W.; Wong, M. W.; Andres, J. L.; Gonzalez, C.; Head-Gordon, M.; Replogle, E. S.; Pople, J. A. *Gaussian 98,* Revision A.5; Gaussian, Inc.: Pittsburgh, PA, 1998.

(120) Becke, A. D. *Phys. Rev. A* **1988**, *38,* 3098.

(121) Perdew, J. P. *Phys. Rev. B: Condens. Matter* **1986**, *33*, 8822.

(122) Dolg, M.; Wedig, U.; Stoll, H.; Preuss, H. *J. Chem. Phys.* **1987**, *86*, 866.

(123) Andrae, D.; Häussermann, U.; Dolg, M.; Stoll, H.; Preuss, H. *Theor. Chim. Acta* **1990**, *77*, 123.

(124) Hehre, W. J.; Ditchfield, R.; Pople, J. A. *J. Chem. Phys.* **1972**, *56*, 2257.

(125) Hariharan, P. C.; Pople, J. A. *Theor. Chim. Acta* **1973**, *28*, 213.

(126) Dunning, T. H. *J. Chem. Phys.* **1971**, *55*, 716.

(127) Dunning, T. H. *J. Chem. Phys.* **1989**, *90*, 1007.

(128) Jonas, V.; Thiel, W. *J. Chem. Phys.* **1995**, *102*, 8474.

(129) Jonas, V.; Thiel, W. *J. Chem. Phys.* **1996**, *105*, 3636.

(130) Jonas, V.; Thiel, W. *J. Phys. Chem. A* **1999**, *103*, 1381.

(131) Mallela, S. P.; Yap, S.; Sams, J. R.; Aubke, F. *Inorg. Chem.* **1986**, *25*, 4237.

(132) Weinstock, B.; Classen, H. H.; Malm, J. G. *J. Am. Chem. Soc.* **1957**, *79*, 5832.

(133) Weinstock, B.; Malm, J. G.; Weaver, E. E. *J. Am. Chem. Soc.* **1961**, *83*, 4310.

(134) von Ahsen, B. Diploma Thesis, Universität Hannover, 1999.

(135) Doherty, N. M.; Hoffman, N. W. *Chem. Rev.* **1991**, *91*, 553.

(136) Murphy, E. F.; Murugavel, R.; Roesky, H. W. *Chem. Rev.* **1997**, *97*, 3425.

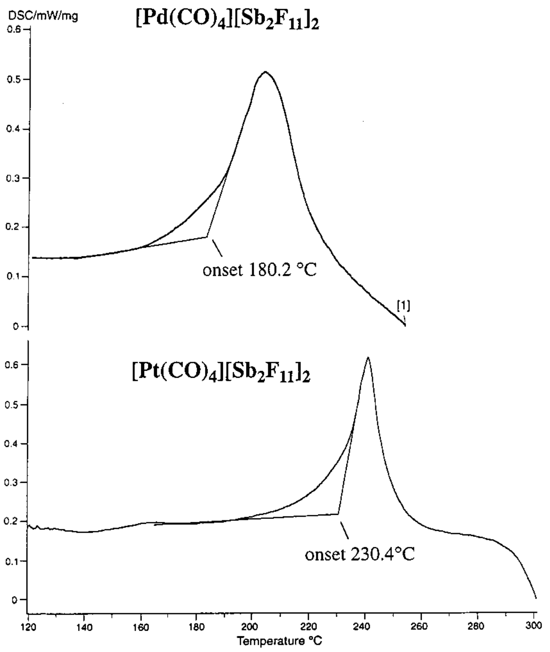

Figure 1. DSC curves in the temperature range of 120−300 °C for $[MCO)_4][Sb_2F_{11}]_2$, M = Pd, Pt.

requires highly reactive and corrosive reagents ($S_2O_6F_2$, F_2). The carbonylation of the commercially available metal dichlorides $PdCl_2$ or $PtCl_2$ in liquid SbF_5[93] seems to provide an alternative. However, the reactions are very slow, proceed in a heterogeneous phase, are suitable for small amounts only, and yield impure products.

Common to all methods discussed here and the synthetic routes to other superelectrophilic[49] carbonyl cation salts is the use of superacids as reaction media, most prominently among them antimony(V) fluoride[48] and more recently HF−SbF_5.[60,61] There are at this time no alternative routes to superelectrophilic metal carbonyl cations and their derivatives.

The compositions of $[M(CO)_4][Sb_2F_{11}]_2$, M = Pd, Pt, are established by the reported microanalyses and the reaction balances.[75] Further extensive characterizations by differential scanning calorimetry, vibrational spectroscopy, ^{13}C MAS NMR spectroscopy, single-crystal X-ray diffraction, and DFT calculations are the subject of this study.

Thermal Behavior of $[M(CO)_4][Sb_2F_{11}]_2$. (a) Observations During the Decomposition Process. Both $[Pd(CO)_4][Sb_2F_{11}]_2$ and $[Pt(CO)_4][Sb_2F_{11}]_2$ are obtained as colorless, very moisture-sensitive solids which show surprisingly high thermal stabilities up to 140 and 200 °C, respectively.[75] When $[Pt(CO)_4][Sb_2F_{11}]_2$ is heated in a glass capillary beyond 200 °C, thermal decomposition occurs, and a black solid (Pt) and a liquid (SbF_5) form. The gas-phase IR spectrum shows only traces of CO. Instead, COF_2 and some CO_2 are observed. The solid residue, after keeping the sample at 220 °C for 3 min, still contains CO bound to Pt. The observed IR bands at 2220 (m) and 2178 (s) cm^{-1} are lower than the E_u mode of $[Pt(CO)_4]^{2+}$ at 2244 $cm^{-1}$and are tentatively attributed to *cis*-$Pt(CO)_2(FSbF_5)_2$.[137] For *cis*-$Pt(CO)_2(SO_3F)_2$ two IR bands of similar intensities are found at 2219 and 2185 cm^{-1} respectively.[71]

(b) Differential Scanning Calorimetry. The results of the DSC measurements for the temperature range of 120−300 °C are shown in Figure 1. As can be seen, the thermal behaviors of both $[Pd(CO)_4][Sb_2F_{11}]_2$ and $[Pt(CO)_4][Sb_2F_{11}]_2$ are similar. An initial small shoulder centered at ∼50 °C, found for both compounds, is followed by endothermic events with onsets at 180 °C and 230 °C for the $[Pd(CO)_4]^{2+}$ and $[Pt(CO)_4]^{2+}$ compounds, respectively. The peak area of ∼60 kJ mol^{-1} is similar for both compounds. The thermal events are not reversible, which argues against a simple melting process. The gaseous products of the decomposition are COF_2 and CO_2 (probably formed by hydrolysis). CO is not observed in either run. The black solid residue with IR bands at 2238(s), 2206(s) and 2167(w) for the Pt complex and 2249(m) ($[Pd(CO)_4]^{2+}$), 2216(m) and 2186 (m) with an additional weak band at 1993 cm^{-1} for the Pd complex are tentatively identified as *cis*-$M(CO)_2(FSbF_5)_2$, M = Pd, Pt, by analogy to *cis*-$M(CO)_2(SO_3F)_2$, M = Pd, Pt,[71] and to observations by C. Wang.[137]

(c) Summary. While the observation of metal (Pd, Pt), liquid SbF_5, and COF_2 suggest two or even three different simultaneous decomposition modes, four conclusions can be drawn from the observations: (i) $[Pt(CO)_4][Sb_2F_{11}]_2$ has greater thermal stability than $[Pd(CO)_4][Sb_2F_{11}]_2$ by about 60 °C, with the latter stable at least to 140 °C and the former to ∼200 °C. (ii) CO is either not observed (DSC measurements) or is formed only in trace amounts. Instead, COF_2 and CO_2 are formed. (iii) The endothermic thermal events appear to be quite similar for both compounds. (iv) In addition to a complete breakdown of $[M(CO)_4][Sb_2F_{11}]_2$, M = Pd, Pt, resulting in metal formation, the decomposition appears to proceed via intermediates such as *cis*-$M(CO)_2X_2$, M = Pd, Pt; X = Sb_2F_{11}, SbF_6.

A very similar decomposition is found for $[Au(CO)_2][Sb_2F_{11}]$ in a glass capillary. Here Au and SbF_5 are formed on heating the sample to about 200 °C, while in the gas phase COF_2 and CO_2 are observed by IR spectroscopy. A distinctly different mode of thermal decomposition has been observed recently for the complex $[Fe(CO)_6][Sb_2F_{11}]_2$.[80] Initially, SbF_5 is released to give $[Fe(CO)_6][SbF_6]_2$, which undergoes at $T = 140-150$ °C an irreversible loss of CO to give previously reported $Fe[SbF_6]_2$.[138] It is very unlikely that a controlled thermal decomposition of $[Pt(CO)_4][Sb_2F_{11}]_2$ will produce such elusive compounds as $Pt[SbF_6]_2$ or PtF_2. The thermal behavior of $[Au(CO)_2][Sb_2F_{11}]$, $[Fe(CO)_6][SbF_6]_2$, and $[M(CO)_4][Sb_2F_{11}]_2$, M = Pd, Pt, is in sharp contrast to that of the silver(I) tetra(teflato)borate CO-adducts $Ag(CO)_nB(OTeF_5)_4$, $n = 0$, 1, 3,[139,140] which undergo facile CO addition and dissociation and are thermally unstable at ambient conditions.

Structural Aspects of $[M(CO)_4][Sb_2F_{11}]_2$, M = Pd, Pt. (a) Crystal Structures of $[M(CO)_4][Sb_2F_{11}]_2$, M = Pd, Pt. The crystallographic data for $[Pd(CO)_4][Sb_2F_{11}]_2$ and $[Pt(CO)_4][Sb_2F_{11}]_2$ are summarized in Table 1. The data are obtained at identical experimental conditions at 180 ± 1 K. The structures are refined in the same manner and nearly identical R (0.025) and R_w (0.048) values are obtained for both salts. As can be seen from the data in Table 1, both $[Pd(CO)_4][Sb_2F_{11}]_2$ and $[Pt(CO)_4][Sb_2F_{11}]_2$ are isostructural. They crystallize in the monoclinic spacegroup $P2_1/c$ (N*o*. 14). Packing of the four formula units in the unit cell, shown in Supporting Information in Figure S2, is identical for both $[M(CO)_4][Sb_2F_{11}]_2$, M = Pd, Pt, salts, and the unit cell dimensions are very similar for both, as seen in Table 1. The unit cell volume of $[Pt(CO)_4][Sb_2F_{11}]_2$ is slightly smaller by 0.4% than that of the Pd(II) complex. Interestingly, for the isostructural pair *cis*-$M(CO)_2(SO_3F)_2$, M = Pd,[72] Pt,[73] where weaker inter- and intramolecular interactions

---

(137) Wang, C. Ph.D. Thesis, University of British Columbia, 1996.

(138) Gantar, D.; Leban, I.; Frlec, B.; Holloway, J. H. *J. Chem. Soc., Dalton Trans.* **1987**, 2379.

(139) van Seggen, D. M.; Hurlburt, P. K.; Noirot, M. D.; Anderson, O. P.; Strauss, S. H. *Inorg. Chem.* **1992**, *31*, 1423.

(140) Hurlburt, P. K.; Rack, J. J.; Luck, J. S.; Dec, S. F.; Webb, J. D.; Anderson, O. P.; Strauss, S. H. *J. Am. Chem. Soc.* **1994**, *116*, 10003.

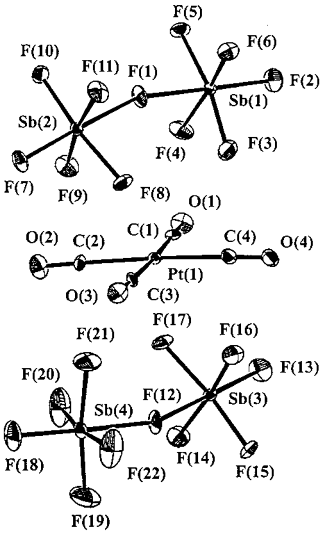

Figure 2. Ortep plot (30% probability ellipsoids) of a formula unit of $[Pt(CO)_4][Sb_2F_{11}]_2$.

Table 2: Selected Bond Parameters for $[M(CO)_4][Sb_2F_{11}]_2$, M = Pd, Pt[a]

	M = Pd	M = Pt
(a) Bond Length [Å]		
Sb(1)−F(1)	2.000(3)	2.011(3)
Sb(2)−F(1)	2.049(3)	2.034(3)
Sb(3)−F(12)	2.015(3)	2.011(3)
Sb(4)−F(12)	2.032(3)	2.034(3)
M(1)−C(1)	1.991(6)	1.984(8)
M(1)−C(2)	2.006(6)	1.980(8)
M(1)−C(3)	1.987(6)	1.987(8)
M(1)−C(4)	1.984(6)	1.979(9)
O(1)−C(1)	1.110(6)	1.086(9)
O(2)−C(2)	1.100(6)	1.106(9)
O(3)−C(3)	1.105(6)	1.110(9)
O(4)−C(4)	1.111(7)	1.118(9)
(b) Bond Angles [deg]		
C(1)−M(1)−C(2)	93.0(2)	92.2(3)
C(1)−M(1)−C(4)	89.6(2)	90.7(3)
C(2)−M(1)−C(3)	88.8(2)	89.8(3)
C(3)−M(1)−C(4)	88.6(2)	87.4(3)
Sb(1)−F(1)−Sb(2)	151.6(2)	153.8(2)
Sb(3)−F(12)−Sb(4)	158.8(2)	161.1(2)
M(1)−C(1)−O(1)	176.3(5)	176.4(7)
M(1)−C(2)−O(2)	177.0(5)	177.1(7)
M(1)−C(3)−O(3)	176.6(5)	178.1(7)
M(1)−C(4)−O(4)	176.1(5)	177.0(7)

[a] Atom labeling differs between two structures, corresponding parameters are presented side-by-side.

are observed, the unit cell volume of *cis*-$Pt(CO)_2(SO_3F)_2$ is larger by 4.1% than that of *cis*-$Pd(CO)_2(SO_3F)_2$.[73]

(b) Internal Bond Parameters for the $[M(CO)_4]^{2+}$, M = Pd, Pt, Cations. A formula unit of $[Pt(CO)_4][Sb_2F_{11}]_2$ is shown in Figure 2 and of $[Pd(CO)_4][Sb_2F_{11}]_2$ in Figure S3. Selected bond lengths and bond angles are collected in Table 2. A close-up look of the $[M(CO)_4]^{2+}$, M = Pd, Pt, cations is shown in the Supporting Information as Figure S4. As can be seen, there are small departures from planarity. There are also similar angular distortions. The C−M−C angles, M = Pd, Pt, for CO ligands *cis* to each other range from 88.6(2) to 93.0(2)° for the Pd(II) cation and from 87.4(3) to 92.3(3)° for $[Pt(CO)_4]^{2+}$. As is commonly found for cationic metal carbonyl complexes, the M−C−O groups, M = Pd, Pt, show a very slight departure from linearity.

Both M−C and C−O distances vary slightly for both cations. The $d(M{-}C)_{av}$ values of 1.992(6) and 1.982(9) Å for $[Pd(CO)_4]^{2+}$ and $[Pt(CO)_4]^{2+}$ are identical within error limits, as are the average C−O distances of 1.106(6) and 1.110(9) Å, respectively. The average M−C, M = Pd, Pt, and C−O distances for both cations together with the average CO stretching wavenumbers $\tilde{\nu}(CO)_{av}$ and the CO stretching force constants f_{CO} are listed in Table 3, where they are compared to the corresponding data for other structurally and spectroscopically characterized Pd(II)- and Pt(II) carbonyl derivatives such as *cis*-$M(CO)_2(SO_3F)_2$, M = Pd, Pt,[71−73] *cis*-$Pt(CO)_2Cl_2$,[5] dinuclear *trans*-$Pt_2(CO)_2I_2(\mu\text{-}I)_2$[141] and three carbonyl trihalide anions of the type $[MCl_3(CO)]^-$, M = Pd,[141] Pt,[142] and $[PdBr_3(CO)]^-$,[141] all with $[NBut_4]^+$ as countercation. All anionic complexes have been previously characterized by vibrational spectroscopy.[22,143]

As can be seen in Table 3, the average M−C distances for the cation $[Pt(CO)_4]^{2+}$ are the longest Pt−C internuclear distances so far reported. Equally unprecedented for Pt(II) carbonyls are the high $\tilde{\nu}(CO)_{av}$ and f_{CO} values. On substitution of two or more CO groups by anionic ligands (SO_3F, Cl, Br, I) the Pt−C distance and the CO bond strength both decrease. The vibrational data ($\tilde{\nu}(CO)_{av}$, f_{CO}) provide a more precise measure of the strength of the CO bond, than do the CO distances, which for all compounds listed in Table 3 are identical within esd values, while the $\tilde{\nu}(CO)_{av}$ wavenumbers are spread over 166 cm^{-1}.

For $[Pd(CO)_4]^{2+}$ not only the M−C distances but also $\tilde{\nu}(CO)_{av}$ and f_{CO} are nearly identical to those of $[Pt(CO)_4]^{2+}$ as discussed above. However, for the isostructural pairs *cis*-$M(CO)_2(SO_3F)_2$[72,73] and $[MCl_3(CO)]^-$,[141,143] M = Pd, Pt, longer M−C bonds and shorter C−O bonds are found for the palladium compounds, in agreement with previous observations.[22,144] These differences, previously noted in isostructural Pd- and Pt carbonyl derivatives,[22,143,144] must be, as recently discussed,[73] due to effects caused by the anionic ligands.

A comparison to tabulated data from the Cambridge data compilation[145] is only possible for the Pt(II) carbonyl species. Compared to the listed mean Pt−C distance of 1.854 Å and the upper quartile q_u value of 1.878 Å, based on 29 samples, the observed average distances for $[Pt(CO)_4][Sb_2F_{11}]_2$ (1.992(6) Å), *cis*-$Pt(CO)_2Cl_2$[5] (1.897(5) Å), and *cis*-$Pt(CO)_2(SO_3F)_2$[73] (1.882(3) Å) are all longer. The CO distances for all compounds listed in Table 3 are at the shorter end of the tabulated data[145] and fall frequently below the lower quartile q_l of 1.132 Å.[145]

A useful structural comparison is possible with the square planar$\{M(CO_{eq})_4\}$ moiety in the structures of $[M(CO)_5Cl][Sb_2F_{11}]_2$, M = Rh, Ir,[78,83] and data for the recently reported cation $[Rh(CO)_4]^+$,[94,95] which is isoelectronic to $[Pd(CO)_4]^{2+}$. For both $[Rh(CO)_4][1\text{-}Et\text{-}CB_{11}F_{11}]$[94] and $[Rh(CO)_4][Al_2Cl_7]$[95] nearly identical average Rh−C distances of 1.951(6)[94] and 1.95(1) Å,[95] respectively, are observed. In addition to similar C−O distances, the $\tilde{\nu}(CO)$ values in the Raman spectra are within 5−10 wavenumbers of each other. It appears, that structural and spectroscopic data for $[Rh(CO)_4]^+$ in both salts[94,95] show a remarkable independence from the counteranion, which in our opinion is due to the absence of significant interionic interactions (vide infra).

---

(141) Andreini, B. P.; Belli Dell'Amico, D.; Calderazzo, F.; Venturi, M. G.; Pelizi, G.; Segre, A. *J. Organomet. Chem.* **1988**, *354*, 357.

(142) Russell, D. R.; Tucker, P. A.; Wilson, S. *J. Organomet. Chem.* **1976**, *104*, 387.

(143) Browning, J.; Goggin, P. L.; Goodfellow, R. J.; Norton, M. G.; Rattray, A. J.; Taylor, B. F.; Mink, J. *J. Chem. Soc., Dalton Trans.* **1977**, 2061.

(144) Belli Dell'Amico, D.; Calderazzo, F.; Zandona, N. *Inorg. Chem.* **1984**, *23*, 137.

(145) Orpen, A. G.; Brammer, L.; Allen, F. H.; Kennard, O.; Watson, D. G.; Taylor, R. *J. Chem. Soc., Dalton Trans.* **1989**, S1.

Table 3: Selected Structural and Vibrational Data for Pd(II) and Pt(II) Carbonyl Complexes

compound	$d(M-C)_{av}$ [Å]	$d(C-O)_{av}$ [Å]	$\tilde{\nu}(CO)_{av}$ [cm^{-1}]	f_{CO}[a] [10^2 N m^{-1}]	ref[b]
$[Pd(CO)_4][Sb_2F_{11}]_2$	1.992(6)	1.106(6)	2259	20.63	*c*, *c*
$[Pt(CO)_4][Sb_2F_{11}]_2$	1.982(9)	1.110(9)	2261	20.64	*c*, *c*
cis-$Pd(CO)_2(SO_3F)_2$	1.932(5)	1.108(6)	2218	19.87	71, 72
cis-$Pt(CO)_2(SO_3F)_2$	1.882(3)	1.116(6)	2202	19.56	71, 73
cis-$Pt(CO)_2Cl_2$	1.897(5)	1.115(6)	2171	18.67	5, 61
trans-$Pt_2(CO)_2I_2(\mu\text{-}I)_2$	1.88(3)	1.06(4)	2106[d]	17.93	141
$[PtCl_3(CO)]^-$ [e]	1.82(1)	1.12(2)	2095	17.74	142, 143
$[PdCl_3(CO)]^-$ [e]	1.87(1)	1.11(1)	2132	18.37	141, 142
$[PdBr_3(CO)]^-$ [e]	1.87(3)	1.10(3)	2120	18.16	141, 142

[a] Approximation according to Cotton and Kraihanzel.[182] [b] Where two references are listed, the first refers to structural data, the second reference refers to vibrational data. [c] This work. [d] Solution in *n*-heptane. [e] $[NBu_4]^+$ as cation.

Table 4: Calculated and Experimental Bond Lengths [Å] and Partial Atomic Charges from Natural Population Analysis[a] for the Isoelectronic Square Planar (D_{4h}) Cations $[M(CO)_4]^{n+}$, M = Co, Rh, Ir, Ni, Pd, Pt, Au, Hg; n = 1, 2, 3, 4, and for Gaseous CO

	experimental		BP86/ECP1		BP86/ECP2						
	d(MC)	d(CO)	d(MC)	d(CO)	d(MC)	d(CO)	q_M	q_C	q_O	q_C+q_O	q_C-q_O
$[Co(CO)_4]^+$	-	-	1.826	1.147	1.829	1.137	−0.08	0.55	−0.28	0.27	0.83
$[Rh(CO)_4]^+$	1.951(6)[b])	1.117(10)[c])	1.965	1.146	1.967	1.135	−0.15	0.56	−0.28	0.29	0.84
$[Ir(CO)_4]^+$	-	-	1.971	1.147	1.972	1.136	−0.12	0.55	−0.27	0.28	0.81
$[Ni(CO)_4]^{2+}$	-	-	1.886	1.136	1.884	1.125	0.50	0.54	−0.16	0.38	0.70
$[Pd(CO)_4]^{2+}$	1.992(6)	1.106(6)	2.015	1.136	2.016	1.125	0.43	0.56	−0.17	0.39	0.72
$[Pt(CO)_4]^{2+}$	1.982(9)	1.110(9)	2.009	1.136	2.009	1.125	0.42	0.55	−0.15	0.39	0.70
$[Au(CO)_4]^{3+}$	-	-	2.081	1.132	2.080	1.121	1.00	0.54	−0.05	0.50	0.59
$[Hg(CO)_4]^{4+}$	-	-	2.278	1.136	2.260	1.124	1.48	0.59	0.04	0.63	0.55
$CO_{(g)}$	-	1.12819[d])	-	1.150		1.138		0.46	−0.46	0.00	0.92

[a] BP86/ECP2 values in units of e. [b] Reference 94. [c] Reference 95. [d] Reference 151.

Slightly longer average M−C distances are found for the four equatorial CO groups in $[Rh(CO)_5Cl]^{2+}$ (2.014(12) Å)[83] and $[Ir(CO)_5Cl]^{2+}$ (2.017(10) Å)[78,83] both with $[Sb_2F_{11}]^-$ as anion. Very slightly shorter Ir−C distances of 2.006(6) and 1.999(6) Å are reported for the *trans*-Ir−$(CO)_2$-segment in *mer*-$Ir(CO)_3(SO_3F)_3$.[146] The $\tilde{\nu}(CO)_{av}$ values for $[Rh(CO)_5Cl]^{2+}$ (2247 cm^{-1}),[83] $[Ir(CO)_5Cl]^{2+}$ (2246 cm^{-1})[78,83] and *mer*-$Ir(CO)_3(SO_3F)_3$ (2213 cm^{-1}),[146] are all lower than $\tilde{\nu}(CO)_{av}$ of 2268 cm^{-1} for $[Ir(CO)_6]^{3+}$ [78,86] with f_{CO} 20.78 × 10^2 N m^{-1}.

It is remarkable how in isostructural pairs such as $[M(CO)_4]^{2+}$, M = Pd, Pt, $[M(CO)_5Cl]^{2+}$, M = Rh, Ir,[78,83] or $[M(CO)_6]^{2+}$, M = Ru, Os,[81,82] the effective radii for the 4d and 5d metal ions appear to be identical, most likely as a result of relativistic effects.[147,148] As a consequence, very similar structural {d(M−C), d(C−O)} and spectroscopic {$\tilde{\nu}(CO)_{av}$, f_{CO}} features are observed within each pair. For the square planar cations $[Rh(CO)_4]^+$,[94,95] $[Pd(CO)_4]^{2+}$, and $[Pt(CO)_4]^{2+}$ the experimental average metal−carbon and carbon−oxygen bond lengths are compared to data from DFT calculations in Table 4. The calculations also include other possibly square planar, homoleptic carbonyl cations such as $[Co(CO)_4]^+$, $[Ir(CO)_4]^+$, $[Ni(CO)_4]^{2+}$, $[Au(CO)_4]^{3+}$, and $[Hg(CO)_4]^{4+}$. Of these, only for $[Co(CO)_4]^+$ and $[Ir(CO)_4]^+$ limited vibrational information is available.[149,150]

As can be seen in Table 4, agreement between experimental and calculated data at two levels of theory is fair. The computed M−C distances are slightly longer, generally by about 0.02 Å. The C−O distances are overestimated by about 0.03 Å at the BP86/ECP1 level and by 0.02 Å at the BP86/ECP2 level, which reflects the corresponding errors for the free CO molecule (see Table 4).[149,151] Similar discrepancies between calculated[96,98−100] and experimental CO distances have been noted for $[Fe(CO)_6]^{2+}$.[80] As the calculated bond parameters are closer to experimental data at the BP86/ECP2 rather than at the BP86/ECP1 level of theory, we shall therefore in the remainder of this paper only discuss the BP86/ECP2 results.

The data for the hypothetical D_{4h} cations $[Au(CO)_4]^{3+}$ and $[Hg(CO)_4]^{4+}$ indicate, that M−C distances increase with increasing ion charge, while CO distances remain in about the same region. It appears unlikely that either of these two cations can be obtained, using presently known synthetic methods. On the other hand $[Co(CO)_4]^+$ and $[Ir(CO)_4]^+$ may have a chance to be prepared. Vibrational evidence for the existence of $[Ir(CO)_4]^+$ in molten $AlCl_3$[149] will be discussed below, and $Co(CO)_4Y$, where Y is an anionic ligand, is recently detected in superacid solution.[150] According to calculations for $[Co(CO)_4]^+$ [152] the triplet state appears to be lower than the singlet state. Collision-induced dissociation studies of $[Co(CO)_n]^+$, n = 1−5,[153] point to the possible existence of $[Co(CO)_5]^+$ which would be isoelectronic to $Fe(CO)_5$.

The structural characterizations of $[M(CO)_4][Sb_2F_{11}]_2$, M = Pd, Pt, reported here, complete a series of data for dipositive metal carbonyl cations with known structures, all obtained as $[Sb_2F_{11}]^-$ or $[SbF_6]^-$ salts. The metals range from group 8 to group 12; all are synthesized in superacids. Their generation involves the four major synthetic methods,[48] (a) solvolytic carbonylation ($[Hg(CO)_2]^{2+}$),[76,77] (b) reductive carbonylation ($[M(CO)_4]^{2+}$, M = Pd, Pt, $[M(CO)_6]^{2+}$, M = Ru, Os),[81,82] (c) oxidative carbonylation ($[Fe(CO)_6]^{2+}$), and (d) oxidation by SbF_5 ($[M(CO)_5Cl]^{2+}$, M = Rh, Ir)[78,83] complemented by the recently discovered conversion of $[M(CO)_6][Sb_2F_{11}]_2$ into $[M(CO)_6][SbF_6]_2$, M = Fe, Ru, Os,[80,82] by elution with anhydrous HF. All salts are thermally stable well above 100 °C.[75−83] Most

---

(146) Wang, C.; Lewis, A. R.; Batchelor, R. J.; Einstein, F. W. B.; Willner, H.; Aubke, F. *Inorg. Chem.* **1996**, *35*, 1279.

(147) Pyykkö, P.; Desclaux, J. P. *Acc. Chem. Res.* **1979**, *12*, 276.

(148) Pyykkö, P. *Chem. Rev.* **1988**, *88*, 563.

(149) Bach, C. Ph.D. Thesis, Universität Hannover, 1998.

(150) Xu, Q.; Inoue, S.; Souma, Y.; Nakatani, H. *J. Organomet. Chem.* **2000**, *606*, 147.

(151) Herzberg, G. *Spectra of Diatomic Molecules*, 2nd ed.; Van Nostrand: Toronto, Canada, 1966; p 521.

(152) Jonas, V., unpublished results.

(153) Goebel, S.; Haynes, C. L.; Khan, F. A.; Armentrout, P. B. *J. Am. Chem. Soc.* **1995**, *117*, 6994 and references therein.

Table 5: Crystallographic, Structural, and Spectroscopic Properties of Selected Superelectrophilic Metal Carbonyl Cations in Their $[Sb_2F_{11}]^-$ or $[SbF_6]^-$ Salts

group	cation	space group	point group	unit cell volume [Å^3]	Z value	d(M−C)$_{av}$ [Å^3]	d(C−O)$_{av}$ [Å^3]	$\tilde{\nu}$(CO)$_{av}$ [cm^{-1}]	$f_{CO}\cdot 10^2$ [N m^{-1}]	ref
12	$[Hg(CO)_2]^{2+}$	$P2_1/n$	D_{4h}	967.1(2)	2	2.083(10)	1.104(12)	2280	21.0	77
10	$[Pd(CO)_4]^{2+}$	$P2_1/c$	D_{4h}	2164.2(4)	4	1.992(6)	1.106(6)	2259	20.63	*a*
	$[Pt(CO)_4]^{2+}$	$P2_1/c$	D_{4h}	2155.7(5)	4	1.982(9)	1.110(9)	2261	20.64	*a*
9	$[Rh(CO)_5Cl]^{2+}$	$P2_1$	C_{4v}	1237.7(2)	2	2.011(10)	1.102(10)	2247	20.41	83
	$[Ir(CO)_5Cl]^{2+}$	$P2_1$	C_{4v}	1226.5(4)	2	2.026(10)	1.086(20)	2246	20.39	83
8	$[Fe(CO)_6]^{2+}$	$P2_1/n$	O_h	1198.4(2)	2	1.911(5)	1.104(6)	2215	19.82	80
	$[Fe(CO)_6]^{2+\,b}$	$P4/mnc$	O_h	850.5(2)	2	1.908(7)	1.108(9)			80
	$[Ru(CO)_6]^{2+}$	$P2_1/n$	O_h	1215.1(2)	2	2.039(5)	1.094(10)	2214	19.80	82
	$[Ru(CO)_6]^{2+\,b}$	$P4/mnc$	O_h	853.1(2)	2	2.024(5)	1.101(7)			82
	$[Os(CO)_6]^{2+}$	$P2_1/n$	O_h	1210.8(2)	2	2.027(5)	1.102(7)	2209	19.71	82
	$[Os(CO)_6]^{2+\,b}$	$P4/mnc$	O_h	850.3(2)	2	2.022(7)	1.104(7)			82

[a] This work. [b] $[SbF_6]^-$-salts, all others $[Sb_2F_{11}]^-$ as anion.

cations are completely characterized by analytical, vibrational,[79−83] NMR, and computational methods[96−98,101−104] in addition to the molecular structure determination by single-X-ray diffraction.[77,78,82,83]

Selected crystallographic, structural, and vibrational data for the fluoroantimonate(V) salts with dipositive metal carbonyl cations are collected in Table 5. They allow some general observations and conclusions: (i) All pairs of salts in groups 9 and 10 are isostructural, as are the members of the two triads in group 8 with either $[Sb_2F_{11}]^-$ or $[SbF_6]^-$ as anions and M = Fe, Ru, Os. As a consequence, crystallographic, structural, and vibrational data within each pair or triad are extremely similar. (ii) The unit cell volume of isostructural compounds decreases from the 4d to the corresponding 5d complexes on average by 0.3 to 0.9% as a consequence of relativistic effects[147,148] and possibly significant interionic, secondary[154] contacts of the C- -F type.[83] (iii) There are in all salts with centro symmetrical cations (point groups $D_{\infty h}$, O_h) very slight departures from ideal geometry, which do not affect the mutual exclusion rule for IR and Raman active fundamentals.[77,80,82] (iv) For the homoleptic carbonyl cations $[M(CO)_n]^{2+}$ in groups 12, 10, and 8 with $n = 2$ (linear), 4 (square planar), or 6 (octahedral), respectively, the strength of the C−O bond, measured as d(C−O)$_{av}$, $\tilde{\nu}$(CO)$_{av}$, and f_{CO}, decreases with increasing n, as the s-orbital contributions to the metal hybrid orbitals of σ-symmetry gradually decrease. The $\tilde{\nu}$(CO)$_{av}$ and f_{CO} values for $[Hg(CO)_2]^{2+}$ [76,77] and $[M(CO)_4]^{2+}$, M = Pd, Pt, together with those for $[Ir(CO)_6]^{3+}$ [78,86] are the three highest sets of values reported to date for metal carbonyl cations.[48] However, the force constants f_{CO} for the three cations, found between 20.63[75] and 21.0×10^2 N m^{-1}, [76,77] are slightly lower than f_{CO} of 21.3×10^2 N m^{-1} calculated for HCO^+,[48,64,76,77] which suggests some residual electron density in π^* molecular orbitals of CO, caused either by π-back-bonding or significant interionic C- -F interactions. (v) Since $[Ir(CO)_6]^{3+}$ [78,86] is not yet structurally characterized and $[Rh(CO)_6]^{3+}$ is still unknown, their monochloropentacarbonyl derivatives $[M(CO)_5Cl]^{2+}$, M = Rh, Ir,[78,83] are included in Table 5. While substitution of a single CO in $[Ir(CO)_6]^{3+}$ by Cl^- results in a slight reduction of $\tilde{\nu}$(CO)$_{av}$ from 2268 to 2247 cm^{-1} and f_{CO} from 20.78 to 20.40×10^2 N m^{-1},[78,83,86] the CO bonds in the cations $[M(CO)_5Cl]^{2+}$, M = Rh, Ir, are still stronger than in the octahedral cations $[M(CO)_6]^{2+}$, M = Ru, Os, as a consequence of the higher oxidation state of the metal ions in the first group of cations.[82]

In summary, the survey presented in Table 5, complemented by similar data for structurally characterized *cis*-$Pt(CO)_2Cl_2$,[5] *cis*-$M(CO)_2(SO_3F)_2$, M = Pd,[71,72] Pt,[71,73] *mer*-$Ir(CO)_3(SO_3F)_3$,[146] and the recently reported group 6 carbonyl cations in the salts $[W(CO)_6(FSbF_5)][Sb_2F_{11}]$[84] and in polymeric $[\{Mo(CO)_4\}(cis\text{-}\mu\text{-}F_2SbF_4)_3]_x[Sb_2F_{11}]_x$[85] establishes the superelectrophilic metal carbonyl cations and their derivatives as a substantial and important group. Even though square planar $M(CO)_4$ species are unknown for neutral carbonyls[5,14−16] and the highly reduced carbonylates,[25] the cations $[M(CO)_4]^{2+}$, M = Pd, Pt, and $[Rh(CO)_4]^+$ [94,95] are now structurally and spectroscopically well characterized and are the subject of theoretical calculations in this study. The vast majority of the superelectrophilic cations have the fluoroantimonate(V) species $[SbF_6]^-$ and $[Sb_2F_{11}]^-$ as counteranions with $[Pt(CO)_4][Pt(SO_3F)_6]$[74] and $[Pt(CO)_4][PtF_6]$[86] notable exceptions. The role of $[Sb_2F_{11}]^-$ in providing thermally stable salts of the $[M(CO)_4]^{2+}$ cations, M = Pd, Pt, is now examined.

(c) The $[Sb_2F_{11}]^-$ ions in $[M(CO)_4][Sb_2F_{11}]_2$. A complete listing of all Sb−F interatomic distances and F−Sb−F bond angles is found in the Supporting Information section. While the Sb−F interatomic distances are unremarkable, the bond angles listed show two abnormalities: (i) F_{ax}−Sb−F_{eq} angles are slightly wider than 90 °C, while F_{eq}−Sb−F_b angles are consequently more acute, by about 5°. It appears that the equatorial fluorine "lean" slightly toward the weakly bonded Sb−F_b−Sb group, in agreement with the VSEPR theory of molecular structure.[155−158] (ii) As will be discussed below, the Sb−F_b−Sb bridge angle α departs significantly from 180°.

With a linear Sb−F_b−Sb moiety, together with eclipsed SbF_4 groups, the di-octahedral anion would be centro symmetrical (point group D_{4h}). The mutual exclusion rule for IR- and Raman active vibrations permits easy detection. The D_{4h} conformer is however quite rare and found in $[H_3F_2][Sb_2F_{11}]$[159] and in the metal carbonyl salts $[Au(CO)_2][Sb_2F_{11}]$,[65,66,134] $[Rh(CO)_4][Sb_2F_{11}]$,[95] and curiously in $[Re(CO)_6][Re_2F_{11}]$[160] where Re has replaced Sb in the anion. In all examples the cations are unipositive. In the structurally characterized carbonyl complexes[134,160] there are no significant interionic interactions in their $[M_2F_{11}]^-$ salts, M = Sb, Re. A bent $[Sb_2F_{11}]^-$ ion is reported recently in a salt of the composition $[Au(CO)_2]_2[SbF_6][Sb_2F_{11}]$[161] and in $[H_2F][Sb_2F_{11}]$.[159]

---

(154) Alcock, N. W. *Adv. Inorg. Radiochem.* **1972**, *15*, 1.

(155) Gillespie, R. J. *Molecular Geometry*; van Nostrand: London, 1972.

(156) Gillespie, R. J.; Hargittai, I. *The VSEPR Model of Molecular Geometry*; Allyn and Bacon: Boston, 1991.

(157) Gillespie, R. J. *J. Chem. Soc. Rev.* **1992**, *22*, 59.

(158) Gillespie, R. J.; Robinson, E. A. *Angew. Chem., Int. Ed. Engl.* **1996**, *35*, 495.

(159) Mootz, D.; Bartmann, K. *Angew. Chem., Int. Ed. Engl.* **1988**, *27*, 391.

(160) Bruce, D. M.; Holloway, J. H.; Russell, D. R. *J. Chem. Soc., Dalton Trans.* **1978**, 1627.

(161) Küster, R.; Seppelt, K. *Z. Anorg. Allg. Chem.* **2000**, *626*, 236.

Table 6: Characteristic Structural Features of the $[Sb_2F_{11}]^-$ Anion in Salts with Metal Carbonyl Cations

cation	point group anion	bridge angle α [°]	dihedral angle ψ [°]	bond lengths in bridge [Å]	ref
$[Au(CO)_2]^+$	D_{4h}	180.0	0	1.979(3); 1.979(3)	134
$[Au(CO)_2]^{+\,a}$	C_1	152.5(3)	n.a.	2.025(2)	161
$[Hg(CO)_2]^{2+}$	C_1	147.6(3)	36.5	2.008(4); 2.035(4)	77
$[Pd(CO)_4]^{2+}$	$\sim C_{2v}$	158.8(2)	9	2.015(3); 2.032(3)	*b*
	C_1	151.64(15)	38	2.000(3); 2.049(3)	*b*
$[Pt(CO)_4]^{2+}$	$\sim C_{2v}$	161.1(2)	0.5	2.013(3); 2.034(3)	*b*
	C_1	153.8(2)	42	2.011(3); 2.038(3)	*b*
$[Rh(CO)_5Cl]^{2+}$	C_1	154.7(6)	31	2.023(9); 1.977(10)	83
	C_1	156.3(5)	41	2.038(9); 1.982(9)	83
$[Ir(CO)_5Cl]^{2+}$	C_1	153.2(6)	34	1.946(9); 2.089(10)	83
	C_1	156.5(6)	49	1.980(10); 2.007(9)	83
$[Fe(CO)_6]^{2+}$	C_1	148.5(2)	38	2.053(3); 1.998(3)	79, 80, *c*
$[Re(CO)_6]^{+\,d}$	D_{4h}	180	0	2.009(2); 2.009(2)	160
$[\{Mo(CO)_4\}_2(F_2SbF_4)_3]^+$	C_1	150.0(3)	19	2.051(6); 2.014(6)	85
$[W(CO)_6(FSbF_5)]^+$	C_1	149.4(3)	30	2.034(5); 2.022(5)	84

[a] $[Sb_2F_{11}]^- \cdot [SbF_6]^-$ as anion. [b] This work. [c] Identical α and ψ angles as well as $Sb-F_b$ distances are found for $[Ru(CO)_6][Sb_2F_{11}]_2$ and $[Os(CO)_6][Sb_2F_{11}]_2$. [d] $[Re_2F_{11}]^-$ as anion.

In most metal carbonyl $[Sb_2F_{11}]^-$ salts, two simultaneous distortions from D_{4h} symmetry are noted:[160] (a) bending about F_b which is expressed in terms of a bridge angle α and (b) rotation of the two $SbF_{4\,eq}$ groups into a staggered conformation expressed in terms of a dihedral angle ψ.[160] Where both rotational and bending processes are present, the $[Sb_2F_{11}]^-$ anion has no symmetry (point group C_1). The C_1 conformation is most commonly encountered. A summary of older examples is found in ref 160. More recent results, obtained mainly by us, are listed in Table 6. In addition to bending and rotational distortion, two minor deformations are noted: (a) a slight asymmetry within the bridge where both $Sb-F_b$ distances are no longer equal and (b) a slight lengthening of the Sb−F bonds where F is involved in secondary bonding.

The crystallographic results for the anions in $[M(CO)_4][Sb_2F_{11}]_2$, M = Pd, Pt, are surprising on three accounts: (i) Both $[Sb_2F_{11}]^-$ anions in both salts are no longer symmetry-related and have different bridge and dihedral angles. This is usually not the case for salts with other centrosymmetrical cations such as $[Hg(CO)_2]^{2+}$ [77] (D_{4h}) or $[M(CO)_6]^{2+}$, M = Fe,[80] Ru,[82] Os,[82] (O_h), where the $[Sb_2F_{11}]^-$ anions have in each case the same bond parameters including the angles α and ψ. (ii) While the internal bond parameters for the two anions in both salts are very similar and often identical within quoted esd values, the bridge angles for both sets of data differ by about 2−3°. (iii) One of the two conformers in each salt has a dihedral angle of 9° (Pd) and 0.5° (Pt), respectively. This implies that departure from D_{4h} symmetry involves primarily bending about the bridging F-atom, but no significant rotation of the two SbF_4 groups. The approximate symmetry of this unique conformation is C_{2v}. Both conformers are shown in Figure S6, taken from the $[Pd(CO)_4][Sb_2F_{11}]_2$ structure. We have argued in the past,[48,63,83] that interionic interactions are the cause of the observed distortions of the $[Sb_2F_{11}]^-$ anions, to strengthen and maximize such interionic contacts. The secondary contacts for $[M(CO)_4][Sb_2F_{11}]_2$, M = Pd, Pt, will be discussed in the next section.

(d) Interionic interactions in $[M(CO)_4][Sb_2F_{11}]_2$, M = Pd, Pt. Significant interionic contacts in superelectrophilic salts are usually of the F- -C-type.[79−85] This is not surprising, since in octahedral[80,82,83] or seven-coordinate[84,85] metal carbonyl cations, the central metal is not accessible for F atoms of the anion. For linear $[Hg(CO)_2]^{2+}$, both significant Hg- -F and C- -F contacts are observed, but Hg- -F contacts are found only in bifurcated fluorine bridges (see Figure S5). The Hg- -F contacts produce a distorted octahedral environment for the central metal by 2:4 coordination. The F- -C contacts in $[Hg(CO)_2][Sb_2F_{11}]_2$ are equally significant and more numerous (10 per cation). The bifurcated interactions, shown in Figure S5, are seen as strengthening the Hg−C bonds, which are already strong on account of relativistic effects.[147,148] They are also important in extending the molecular structure into a three-dimensional framework.[77] An illustration of the coordination environments of carbon and mercury in $[Hg(CO)_2][Sb_2F_{11}]_2$[77] may be found in Figure 4 of ref 48.

It seems the “open” square planar structures of the $[M(CO)_4]^{2+}$ cations (see Figure S4) with point group D_{4h} in the salts $[M(CO)_4][Sb_2F_{11}]_2$ become interesting test cases, because the formation of secondary M- -F, M = Pd, Pt, and C- -F contacts are both possible for stereochemical reasons. To assist in the discussion, we have listed in Table 4 the partial charges calculated from natural population analysis for square planar $[M(CO)_4]^{n+}$, M = Rh, Ir, Ni, Pd, Pt, Au, Hg, all with d^8 configurations, and $n = 1$ to 4. As can be seen, for $[M(CO)_4]^{2+}$, M = Pd, Pt, both M and C are positively charged. The calculated partial charges on the four C-atoms (0.56 or 0.55) are slightly higher than those for Pd (0.43) and Pt (0.44), which would favor C- -F over M- -F contacts.

To judge the strength of the interionic contacts, we have chosen to use the van der Waals radii of Bondi.[162] It is convenient to arbitrarily classify those contacts, which are equal or shorter than the sum of the van der Waals radii[162] by 10% or more as “significant” and those between this “significance” limit and the sum of the van der Waals radii as “marginal”. For C- -F interactions, the corresponding contact distances are 2.85 and 3.17 Å, respectively.[162]

The relevant sums of van der Waals radii are summarized in Table S1, where the observed M- -F and C- -F interionic contacts are listed. In addition a number of relatively long F- -F and O- -F contacts are observed, which are seemingly due to repulsive interactions. Occasionally marginal O- -F contacts are observed in bifurcated interactions together with stronger C- -F contacts for the same carbonyl group. The M- -F and C- -F contacts for Pd, Pt, and each of the four carbon atoms (C(1) to C(4)) are listed in order of decreasing strength. Also listed for each carbon atom are $d(C\text{- -}F)_{av}$ values for those contacts, that are shorter than the sum of the van der Waals radii (3.17 Å). Since a different numbering system is used for both $[M(CO)_4]^{2+}$ cations, M = Pd, Pt, individual data are not directly comparable. The secondary[154] interionic contacts for a formula unit of

---

(162) Bondi, A. *J. Phys. Chem.* **1964**, *68*, 441.

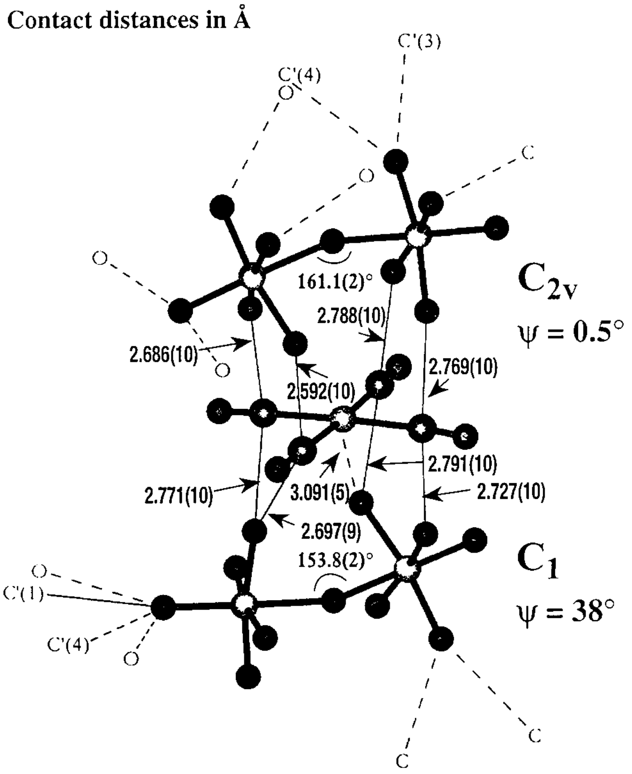

Figure 3. Significant and marginal secondary contacts within a formula unit of $[Pt(CO)_4][Sb_2F_{11}]_2$.

$[Pt(CO)_4][Sb_2F_{11}]_2$ are shown in Figure 3. An identical arrangement due to secondary contacts is found for $[Pd(CO)_4][Sb_2F_{11}]_2$.

The following conclusions are reached: (i) The interionic interactions observed for $[M(CO)_4][Sb_2F_{11}]_2$, M = Pd, Pt, are almost exclusively of the C- -F type. They contribute, as can be seen in Figures 3 and S2, to tight packing of anions and cations in the unit cell, as well as to the formation of extended structures. (ii) There are for each of the four CO-groups four to five C- -F interactions. Of these approximate 20 contacts, eight—two for each carbon—are termed "significant" (between 2.592(10)−2.791(10) Å). They are involved in direct C- -F contacts within a formula unit as seen in Figure 3. Additional borderline or marginal contacts reflect interionic interactions to adjacent $[Pt(CO)_4]^{2+}$ cations (see Figure S2 for the packing arrangement within the unit cell) and aid in the formation of extended structures. (iii) There is in each salt only a single, very marginal M- -F contact, M = Pd, Pt, which is formed as a bifurcated M- -F- -C interaction together with a significant C- -F contact. There is in the $[M(CO)_4][Sb_2F_{11}]_2$ salts, M = Pd, Pt, no evidence for a coordination expansion of the metal from 4 to 6 (termed 4:2 coordination), which is frequently found, for example, in related square planar gold(III) complexes such as AuF_3,[163] $Au(SO_3F)_3$,[164] or $Au[AuF_4]_2$[165] in their solid-state structures. (iv) The strength of the interionic C- -F contacts in both $[M(CO)_4][Sb_2F_{11}]_2$, M = Pd, Pt, salts is very similar. The shortest contact of 2.591(10) Å is found for the Pt(II) salt, closely followed by a C- -F contact of 2.613(7) Å for the Pd(II) complex; however the average C- -F contacts are with 2.865 (Pt) and 2.866 (Pd) Å identical for both salts. (v) With very similar internal bond parameters for both cations (see Table 2) and the four anions in both salts, as well as nearly identical interionic contacts, it is difficult to state clearly, why $[Pt(CO)_4][Sb_2F_{11}]_2$ has a smaller unit cell volume than $[Pd(CO)_4][Sb_2F_{11}]_2$ (see Table 1 or 5). The only discernible differences in the two salts are the slightly wider $Sb-F_b-Sb$ bridge angles α in both conformers (about 2.0−2.5°) and smaller dihedral angle ψ of the C_{2v} form of the $[Sb_2F_{11}]^-$ anion in the Pt(II) compound, which allow for very slightly tighter packing. In any event, the very small contraction in unit cell volume by 0.4% appears to be due to very subtle structural differences between both $[M(CO)_4][Sb_2F_{11}]_2$, M = Pd, Pt, salts. (vi) As can be seen in Figure 3 all eight significant C- -F interactions involve only equatorial F-atoms of the anions. The unprecedented C_{2v} conformation of the $[Sb_2F_{11}]^-$ anion is ideally suited to form four significant C- -F contacts to match the four C atoms of the square planar $[M(CO)_4]^{2+}$ cation, M = Pd, Pt. In the staggered C_1 conformer, F(21) forms two very strong bifurcated contacts (2.771(10) and 2.697(10) Å) to C(2) and C(3), while the adjacent F(18) atom is involved in slightly longer contacts (2.848(9) and 2.889(9) Å) to C′(1) and C′(4) atoms of a neighbor cation (see Figure 3). (vii) The involvement of all four C-atoms of the $[M(CO)_4]^{2+}$ cations, M = Pd, Pt, in forming four to five secondary interionic contacts, explains the relatively high thermal stabilities of the salts.

It is tempting to attribute the observed formation of COF_2 during the thermal decomposition of $[M(CO)_4][Sb_2F_{11}]_2$ (vide supra) to the existence of C- -F contacts in the solid-state structures of the salts, but at the decomposition temperatures of 150−200 °C fluorination of CO by SbF_5 is a possibility[166] as well. In contrast to these observations, for several polycarbonyl adducts of Ag(I) and Cu(I),[42,43,140,167] the reversible dissociation and re-addition of CO has been observed at ambient conditions.

Extended structures are also found for the square planar isostructural molecular complexes *cis*-$M(CO)_2(SO_3F)_2$, M = Pd,[72] Pt,[73] and *cis*-$Pt(CO)_2Cl_2$[5] which are all structurally characterized. For example, for *cis*-$Pd(CO)_2(SO_3F)_2$,[72] four inter- or intramolecular C- -O contacts in the range of 2.839(6)−3.172(6) Å are found for each CO group with only a single marginal Pd- -O interlayer contact of 3.007(4) Å.[72] In *cis*-$Pt(CO)_2Cl_2$[5] the square planar molecules are stacked into columns by intermolecular C- -Cl contacts. In all instances,[5,72,73] the observed secondary contacts are weaker and less numerous than they are in the $[M(CO)_4][Sb_2F_{11}]_2$ salts, M = Pd, Pt.

For $[Rh(CO)_4][Al_2Cl_7]$,[95] the shortest long-range C- -Cl contact is with 3.366 Å just barely below the sum of the van der Waals radii[162] of 3.45 Å, while the shortest Rh- -Cl contact of 3.746 Å is longer than 3.40 Å, estimated as the sum of the van der Waals radii.[162] Significant interactions are, as stated above, commonly absent in metal carbonyl salts with complex charges of +1 or less, as in linear $[Au(CO)_2][Sb_2F_{11}]$[67,134] and octahedral $[Re(CO)_6][Re_2F_{11}]$.[160] For the recently synthesized compound $[Rh(CO)_4][Sb_2F_{11}]$[95] the vibrational analysis suggests D_{4h} symmetry for both the cation and the anion. This is suggestive of the absence of significant interionic interactions.

For $[Rh(CO)_4][1\text{-Et-}CB_{11}F_{11}]$[94] the only interionic interactions listed are a single Rh- -H contact of 3.21 Å and 5 Rh- -F contacts for the formula unit in the range of 3.220(9)−3.588(9) Å which are claimed to affect $\tilde{\nu}(CO)_{av}$ relative to matrix isolated $[Rh(CO)_4]^+$.[168−170] However, all secondary interionic contacts to rhodium listed[94] are longer than the sum of the van der Waals

---

(163) Einstein, F. W. B.; Rao, P. R.; Trotter, J.; Bartlett, N. *J. Chem. Soc. A* **1967**, 478.

(164) Willner, H.; Rettig, S. J.; Trotter, J.; Aubke, F. *Can. J. Chem.* **1991**, *69*, 391.

(165) Schmidt, R.; Müller, B. G. *Z. Anorg. Allg. Chem.* **1999**, *625*, 605.

(166) Emeléus, H. J.; Wood, J. F. *J. Chem. Soc.* **1948**, 2183.

(167) Strauss, S. H. *J. Chem. Soc., Dalton Trans.* **2000**, 1.

(168) Zhou, M. F.; Andrews, L. *J. Phys. Chem. A* **1999**, *103*, 7773.

(169) Zhou, M. F.; Andrews, L. *J. Am. Chem. Soc.* **1999**, *121*, 9141.

(170) Zhou, M. F.; Andrews, L. *J. Chem. Phys.* **1999**, *111*, 4548.

radii[162] and are seemingly not due to attractive interactions.[94] In $[Rh(CO)_4][1\text{-}Et\text{-}CB_{11}F_{11}]$ there are also 14 marginal C- -F contacts, three or four for each CO, between 2.926 and 3.155 Å, which are all shorter than the sum of the van der Waals radii of 3.17 Å.[162] These contacts have been omitted by the authors,[94] but are more likely to affect $\tilde{\nu}(CO)_{av}$ than the long Rh- -F contacts.

In summary the interionic C- -F contacts observed for $[M(CO)_4][Sb_2F_{11}]_2$, M = Pd, Pt, here are stronger and more numerous than in other $[Sb_2F_{11}]^-$ salts of superelectrophilic metal carbonyl cations such as $[Hg(CO)_2]^{2+}$,[77] $[M(CO)_5Cl]^{2+}$, M = Rh, Ir,[78,83] and $[M(CO)_6]^{2+}$, M = Fe, Ru, Os.[80,81,82] With the exception of the four Hg- -F contacts already discussed, there is no evidence for other than occasional, very marginal single M- -F contacts in any of the above-mentioned superelectrophilic metal carbonyl salts as well as in the structures of $[Au(CO)_2][Sb_2F_{11}]$,[67,134] $[Au(CO)_2]_2[Sb_2F_{11}\cdot SbF_6]$,[161] $[Re(CO)_6][Re_2F_{11}]$,[160] $[W(CO)_6(FSbF_5)][Sb_2F_{11}]$,[84] polymeric$[\{Mo(CO)_4\}_2$ $(cis\text{-}\mu\text{-}F_2SbF_4)_3]_x[Sb_2F_{11}]_x$,[85] $[M(CO)_6][SbF_6]_2$, M = Fe, Ru, Os,[80,81,82] and, using accepted criteria, in $[Rh(CO)_4][1\text{-}Et\text{-}CB_{11}F_{11}]$.[94] Similarly there are no significant M- -O contacts in the fluorosulfates *cis*-$M(CO)_2(SO_3F)_2$, M = Pd,[72] Pt,[73] and *mer*-$Ir(CO)_3(SO_3F)_3$[146] nor are there significant M- -Cl contacts in the metal carbonyl chlorides *cis*-$Pt(CO)_2Cl_2$,[5] $Au(CO)Cl$[171] and the salt $[Rh(CO)_4][Al_2Cl_7]$.[95] The frequently observed significant C- -X, X = F, O, Cl, contacts are found in predominantly σ-bonded metal carbonyl cations, in agreement with views on the strongly polarized C−O group in these cations.[172]

While we know of no occasion where in thermally stable cationic metal carbonyl salts M- -X, X = F, Cl, O, interactions play a significant or dominant role, we also know of no instance where in metal carbonyls of limited thermal stability, which readily lose CO, like the polycarbonyls of silver(I) or copper(I),[42,167,173] or the recently reported adducts of the type $[HB(3.5\cdot(CF_3)_2pz)_3]M(CO)$, pz = pyrazol; M = Cu, Ag, Au,[174−176] any significant secondary contacts to carbon of the CO ligand are reported.

The presence of electrophilic carbon centers and the generation in superacid media establish a strong link between the superelectrophilic[49] metal carbonyl cations such as $[M(CO)_4]^{2+}$, M = Pd, Pt, discussed here and the large family of carbocations.[50] There is a recent example[177] where fluoro-substituted carbocations are stabilized by $[As_2F_{11}]^-$ to form stable compounds with the anion in a $\sim C_1$ conformation similar to the conformation of the $[Sb_2F_{11}]^-$ anion commonly encountered in metal carbonyl cations[77,80,83−85] (see Table 6).

Spectroscopic Characterization of $[M(CO)_4]^{n+}$, M = Rh, Ir, Pd, Pt; *n* = 1, 2. (a) Vibrational Spectroscopy. For square planar cations of the type $[M(CO)_4]^{n+}$, M = Rh, Ir, Pd, Pt; *n* = 1 or 2, the irreducible representations of fundamental vibrations and their activities are:

$$\Gamma_{vib} = 2\,A_{1g}\,(Ra, p) + A_{2g}\,(-) + 2\,A_{2u}\,(IR) + 2\,B_{1g}\,(Ra, dp) + 2\,B_{2g}\,(Ra, dp) + 2\,B_{2u}\,(-) + E_g\,(Ra, dp) + 4\,E_u\,(IR)$$

with seven Raman active, six IR active and three inactive vibrational fundamentals. Of the 13 observable fundamentals, only the three CO-stretching vibrations for $[M(CO)_4]^{2+}$, M = Pd,[75] Pt,[74,75,86] and $[M(CO)_4]^+$, M = Rh,[94,149,151] Ir,[149] have been previously reported and have been discussed in the preceding section. In this study, we have made use of the salts $[Pd(CO)_4][Sb_2F_{11}]_2$,[75] $[Pt(CO)_4][Sb_2F_{11}]_2$,[75] $[Pt(CO)_4][Pt(SO_3F)_6]$,[74] $[Pt(CO)_4][PtF_6]$,[86] $[Rh(CO)_4][Sb_2F_{11}]$,[95] and $[Rh(CO)_4][Al_2Cl_7]$[95] as well as their ^{13}C-isotopomers, to arrive at a reasonably complete set of vibrational data for the $[M(CO)_4]^{n+}$ cations, M = Pd, Pt (*n* =2), Rh (*n* = 1).

The vibrational wavenumbers for the salts $[M(CO)_4][Sb_2F_{11}]_2$, M = Pd, Pt, are listed in Table 7. The IR and Raman spectra for $[Pd(CO)_4][Sb_2F_{11}]_2$ and $[Pt(CO)_4][Sb_2F_{11}]_2$ are depicted in Figures 4 and 5. As can be seen, the spectra in the range of 720−500 and 320−200 cm^{-1} are dominated by bands due to the $[Sb_2F_{11}]^-$ anion. This is not unexpected, because the two anions in both salts are of low symmetry (C_1 or $\sim C_{2v}$) and are not symmetry-related. In contrast the $[Sb_2F_{11}]^-$ ions in $[Au(CO)_2][Sb_2F_{11}]$[67] and in $[Rh(CO)_4][Sb_2F_{11}]$[95] have D_{4h} symmetry and only three Raman and three IR bands are observed for the anion with no coincidences.

Due to the unique nature of square planar $M(CO)_4$ moieties in metal carbonyl chemistry[14−17,25] there are no isoelectronic and isosteric metal carbonyl complexes, which could serve as precedents for $[M(CO)_4]^{2+}$, M = Pd, Pt, in a manner similar to $M(CO)_6$, M = Cr, Mo, W, or $[Re(CO)_6]^+$, which have all been completely characterized by various vibrational methods.[178−180] A comparison with these species is very useful in the vibrational analyses of the cations $[M(CO)_6]^{2+}$, M = Fe,[80] Ru, Os,[82] where all vibrational modes are experimentally detected. It is hence not surprising, that only 10 of the 13 observable fundamentals for $[M(CO)_4]^{2+}$, M = Pd, Pt, are identified and assigned. This is similar to the situation for the isoelectronic cyano anions $[M(CN)_4]^{2-}$, M = Pd, Pt,[178,181] where, due to solvent interference and cation dependency of vibrational modes, assignments are incomplete and occasionally ambiguous.[178]

For the isostructural pair $[M(CO)_4][Sb_2F_{11}]_2$, M = Pd, Pt, three interesting observations are made: (i) The intensities of the cation bands in the IR spectra relative to those due to the anions are higher for the platinum compound than for its palladium analogue (see Figures 4 and 5), in accordance also with calculated band intensities (Table S3). In addition, the separations between the three CO stretching modes ν_1, ν_6, and ν_{13} are slightly wider for the Pt complex (22 and 23 cm^{-1}) than for the Pd compound (15 and 14 cm^{-1}). These observations suggest a stronger ionic contribution to the Pd−C bond relative to those for the Pt−C bond. (ii) While $\tilde{\nu}(CO)_{av}$ and f_{CO} values for both cations are very similar, there are large variations in the skeletal vibrations. The M−C stretching modes ν_2, ν_7, and ν_{15} and two of the M−C−O deformation modes are all higher for $[Pt(CO)_4]^{2+}$ than for $[Pd(CO)_4]^{2+}$. (iii) The totally symmetric A_{1g} CO-stretching mode is also observed in the IR spectra of both cations as a weak band. The break-down of the mutual exclusion rule appears to be due to the observed small departure from 90° C−M−C angles and from planarity (Figure S4), due

---

[171] Jones, P. G. *Z. Naturforsch., B: Chem. Sci.* **1982**, *37*, 823.

[172] Goldman, A. S.; Krogh-Jesperson, K. *J. Am. Chem. Soc.* **1996**, *118*, 12159.

[173] Rack, J. J.; Webb, J. D.; Strauss, S. H. *Inorg. Chem.* **1996**, *35*, 277.

[174] Dias, H. V. R.; Lu, H.-L. *Inorg. Chem.* **1995**, *35*, 5380.

[175] Dias, H. V. R.; Jin, W. *J. Am. Chem. Soc.* **1995**, *117*, 11381.

[176] Dias, H. V. R.; Jin, W. *Inorg. Chem.* **1996**, *35*, 3694.

[177] Christe, K. O.; Zhang, X.; Bau, R.; Hegge, J.; Olah, G. A.; Prakash, G. K. S.; Sheehy, J. A. *J. Am. Chem. Soc.* **2000**, *122*, 481 and references therein.

[178] Jones, L. H. *Inorganic Vibrational Spectroscopy*; Marcell Decker: New York, 1971; Vol. 1, p 129.

[179] Jones, L. H.; McDowell, R. S.; Goldblatt, M. *Inorg. Chem.* **1969**, *8*, 2349.

[180] Abel, E. W.; McLean, R. A. N.; Tyfield, S. P.; Braterman, P. S.; Walker, A. P.; Hendra, P. J. *J. Mol. Spectrosc.* **1969**, *30*, 29.

[181] Sweeny, D. M.; Nakagawa, I.; Mizushima, S.; Quagliano, J. V. *J. Am. Chem. Soc.* **1956**, *78*, 889.

[182] Cotton, F. A.; Kraihanzel, C. S. *J. Am. Chem. Soc.* **1962**, *84*, 4432.

Table 7: Observed Vibrational Wavenumbers (cm^{-1}) for $[M(CO)_4][Sb_2F_{11}]_2$, M = Pd,Pt and Estimated Band Intensities, Assignment, and Description of Vibrational Modes

$[Pd(CO)_4][Sb_2F_{11}]_2$				$[Pt(CO)_4][Sb_2F_{11}]_2$				assignments			description
IR	int	Ra	int	IR	int	Ra	int		$[M(CO)_4]^+$	D_{4h}	$[Sb_2F_{11}]^-$
2278	(vw)[a]	2278	(vs)	2288	(vw)	2289	(vs)	ν_1	A_{1g}	$\nu_s(CO)$[b]	
		2263	(s)			2267	(s)	ν_6	B_{1g}	$\nu_{as}(CO)$	
2249	(vs)			2244	(vs)			ν_{13}	E_u	$\nu_{as}(CO)$	
2207	(w)			2204	(w)			ν_{13}'	E_u	$\nu_{as}(^{13}CO)$	
718	(sh)	714	(w)	712	(vs)	714	(w)				$\nu(SbF_{ax})$
708	(vs)	709	(sh)			704	(w)				
		697	(w)			695	(w)				
690	(vs)			689	(vs)						$\nu(SbF_{4eq})$
		686	(m)			686	(m)				
675	(s)			674	(s)						
662	(s)	668	(s)	664	(s)	668	(m)				
		656	(s)			657	(s)				
648	(sh)	649	(s)	648	(sh)	649	(m)				
604	(vw)	598	(w)	604	(sh)	594	(w)				
596	(w)	585	(w)	596	(w)	587	(w)				
503	(m)			502	(w)						$\nu(SbFSb)$
484	(m)			518	(s)			ν_{14}	E_u	$\delta(MCO)$	
		437	(vw)			n.o.		ν_8	B_{2g}	$\delta(MCO)$	
427	(m)			473	(s)			ν_4	A_{2u}	$\delta(MCO)$	
		383	(w)			436	(w)	ν_2	A_{1g}	$\nu_s(MC)$	
		363	(vw)			408	(vw)	ν_7	B_{1g}	$\nu_{as}(MC)$	
336	(sh)			360	(w)			ν_{15}	E_u	$\nu_{as}(MC)$	
		n.o.				341	(vw)	ν_{12}	E_g	$\delta(MCO)$	
315	(s)			313	(s)						$\delta(SbF_{ax})$
305	(s)	305	(m)	305	(m)	304	(m)				
		275	(w)			277	(w)				
267	(vs)			268	(vs)						$\delta(SbF_{eq})$
250	(sh)			250	(vs)						
228	(sh)	230	(m)	228	(sh)	231	(m)				
196	(vw)	201	(vw)	197	(vw)	201	(vw)				
136	(vw)	135	(m)	134	(vw)	139	(m)				$\delta(FSbF)$
		95	(m)			99	(m)	ν_9	B_{2g}	$\delta(CMC)$	

[a] w = weak, m = medium, s = strong, v = very, sh = shoulder. [b] s = symmetric, as = asymmetric, ν = stretching mode, δ = deformation mode.

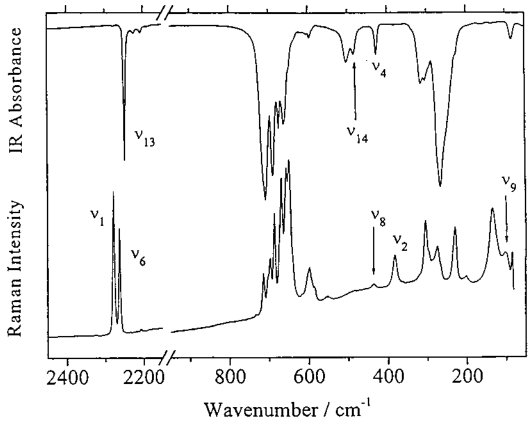

Figure 4. The IR and Raman spectra for $[Pd(CO)_4][Sb_2F_{11}]_2$.

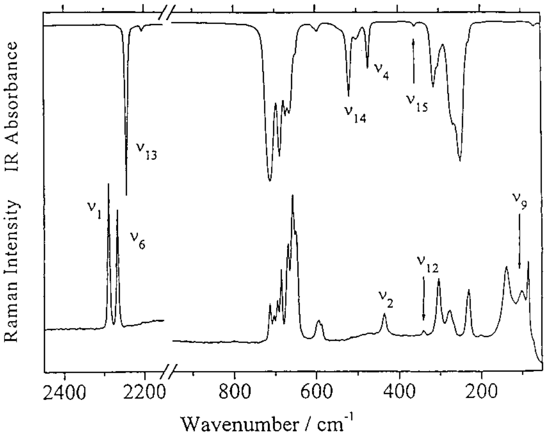

Figure 5. The IR and Raman spectra for $[Pt(CO)_4][Sb_2F_{11}]_2$.

to secondary contacts in both salts and the presence of two different $[Sb_2F_{11}]^-$ anions in both compounds. In contrast for $[M(CO)_6][Sb_2F_{11}]_2$ and $[M(CO)_6][SbF_6]_2$, M = Fe,[80] Ru, Os,[82] secondary interionic contacts are weaker and less numerous than here. The anions are symmetry-related, and no departure from O_h symmetry is noted in the vibrational spectra.[79−82]

The experimental and calculated vibrational wavenumbers for the square planar cations $[M(CO)_4]^{n+}$, M = Rh, Pd, Pt; n = 1, 2, are listed in Table 8. The assignments are supported by experimental and calculated ^{13}C isotope shifts (Table S2) and intensities of IR and Raman bands (Table S3). The inclusion of data for $[Rh(CO)_4]^+$ is warranted, as a result of the vibrational analysis of $[Rh(CO)_4][Sb_2F_{11}]$[95] and $[Rh(CO)_4][Al_2Cl_7]$,[95] where 9 of the observable 13 vibrational fundamentals are detected. For $[Ir(CO)_4]^+$; however, the vibrational information is at present limited to two Raman lines in the CO stretching range, which are observed on melts in $AlCl_3$ (Table S4).[149]

As can be seen in Table S3 the “missing” fundamentals are of rather low calculated intensities (e.g., ν_5 (A_{2u}), ν_8 (B_{2g}), or ν_{16} (E_u)) or are like ν_{12} (E_g) for $[Pd(CO)_4]^{2+}$, seemingly obscured by anion bands. Since $[Pd(CO)_4]^{2+}$ is only stabilized by $[Sb_2F_{11}]^-$, unlike $[Pt(CO)_4]^{2+}$ [74,75,86] or $[Rh(CO)_4]^+$,[94,95] avoidance of anion interference is not possible. In addition to their predicted low intensities, ν_5, ν_9, and ν_{16} are expected to fall below 100 cm^{-1}, which makes their observation difficult.

As can be seen in Table 8, agreement between experimental and calculated band positions is reasonable, considering that

Table 8: Experimental and Calculated Vibrational Wavenumbers (cm^{-1}) for the Square Planar (D_{4h}) Cations $[M(CO)_4]^{n}+$ (M = Rh, Pd, Pt)

cation:			$[Rh(CO)_4]^+$			$[Pd(CO)_4]^+$			$[Pt(CO)_4]^+$		
vibrational modes			expt[a]	calcd	$\Delta\nu$	expt[a]	calcd	$\Delta\nu$	expt[a]	calcd	$\Delta\nu$
ν_1	A_{1g}	ν(CO)	2214	2198	−16	2278	2258	−20	2289	2265	−24
ν_2	A_{1g}	ν(MC)	406[c]	423	+17	383	374	−9	436	424	−12
ν_3	A_{2g}	δ(MCO)	(i.)[d]	320		(i.)	305		(i.)	325	
ν_4	A_{2u}	δ(MCO)	465	437	−28	427	424	−3	473	469	−4
ν_5	A_{2u}	δ(CMC)	n.o.[d]	54		n.o.	85		n.o.	83	
ν_6	B_{1g}	ν(CO)	2174	2150	−24	2263	2236	−27	2267	2237	−30
ν_7	B_{1g}	ν(MC)	406[c]	404	−2	363	349	−14	408	399	−9
ν_8	B_{2g}	δ(MCO)	n.o.	481		437	432	−5	n.o.	462	
ν_9	B_{2g}	δ(CMC)	n.o.	91		95	90	−5	99	96	−3
ν_{10}	B_{2u}	δ(MCO)	(i.)	430		(i.)	407		(i.)	444	
ν_{11}	B_{2u}	δ(CMC)	(i.)	30		(i.)	56		(i.)	56	
ν_{12}	E_g	δ(MCO)	306	316	+10	n.o.	298		341	319	−22
ν_{13}	E_u	ν(CO)	2137	2119	−18	2249	2221	−28	2244	2216	−28
ν_{14}	E_u	δ(MCO)	543	545	+2	484	482	−2	518	513	−5
ν_{15}	E_u	ν(MC)	331	353	+22	336	330	−6	360	340	−20
ν_{16}	E_u	δ(CMC)	n.o.	86		n.o.	93		n.o.	95	

[a] $[Sb_2F_{11}]^-$ salt, ref 95. [b] $AlCl_3$ melt, ref 149. [c] ν_2 and ν_7 are accidentally degenerated. [d] Abbreviations: n.o. = not observed; i. = inactive mode.

Table 9: Calculated and Experimental C−O and M−C Force Constants $f[10^2\ N\ m^{-1}]$ for Square Planar $[M(CO)_4]^{n+}$ Cations

cation	f_{CO} experimental[a]	f_{CO} BP86/ECP2[b]	f_{MC} BP86/ECP2[b]
$[Rh(CO)_4]^+$	19.00	18.50	2.18
$[Ir(CO)_4]^+$		18.39	2.69
$[Ni(CO)_4]^{2+}$		19.75	1.73
$[Pd(CO)_4]^{2+}$	20.63	19.86	1.73
$[Pt(CO)_4]^{2+}$	20.64	19.79	2.20
$[Au(CO)_4]^{3+}$		20.29	1.76
$[Hg(CO)_4]^{4+}$		19.62	0.80

[a] Calculated according to the Cotton−Kraihanzel approximation.[182] [b] Harmonic force constants from ref 130.

the calculations refer to isolated cations and do not account for the role interionic contacts play. Some of the deviations are systematic and reflect well-documented trends in BP86/ECP2 results:[98−100,128−130] for example, CO-stretching frequencies in transition metal carbonyls are on average underestimated by 28 cm^{-1} at this level,[98−100] which reflects a similar error for the free CO molecule.[128] For the salts $[M(CO)_4][Sb_2F_{11}]_2$, M = Pd, Pt, the difference between calculated and experimental wavenumbers, expressed as $\Delta\nu$, falls between −2 and −30 cm^{-1}. In other $[Sb_2F_{11}]^-$ salts with cations such as $[M(CO)_5Cl]^{2+}$, M = Rh, Ir,[83] or $[M(CO)_6]^{2+}$, M = Fe,[79,80] Ru, Os,[81,82] ν(CO)-stretching vibrations are also observed at wavenumbers higher than the calculated values.[83,98−100]

For the three $[Pt(CO)_4]^{2+}$ salts an interesting anion dependency is noted in the CO-stretching region: $[Pt(CO)_4][Sb_2F_{11}]_2$,[75] Ra, 2289, 2267 cm^{-1} IR, 2244 cm^{-1}, $\tilde{\nu}(CO)_{av}$ 2261 cm^{-1}; $[Pt(CO)_4][Pt(SO_3F)_6]$,[74] Ra 2281, 2257 cm^{-1}, IR, 2235 cm^{-1} $\tilde{\nu}(CO)_{av}$, 2252 cm^{-1}; $[Pt(CO)_4][PtF_6]$[86] Ra 2276, 2248 cm^{-1}, IR 2223 cm^{-1} with $\tilde{\nu}(CO)_{av}$ 2242.5 cm^{-1}. With increasing nucleophilicity of the anion,[131] all three CO stretches and $\tilde{\nu}(CO)_{av}$ decrease by about 10 cm^{-1}. Of interest in this context are recent matrix isolation studies,[168−170] where $\tilde{\nu}$(CO) in the IR spectrum of matrix isolated (Ne) $[Rh(CO)_4]^+$ is found at 2162 cm^{-1},[170] compared to 2137 cm^{-1} in $[Rh(CO)_4][Sb_2F_{11}]$.[95] Therefore the $\tilde{\nu}$(CO) values in BP86/ECP2 calculations are possibly even more underestimated than indicated by the data in Table 8.

To summarize some of the observed trends, experimental and calculated force constants are listed in Table 9. While f_{CO} values for the two pairs of 4d and 5d cations remain reasonably constant, the f_{MC} values for $[Rh(CO)_4]^+$ and $[Pd(CO)_4]^{2+}$ are substantially lower than those for $[Ir(CO)_4]^+$ and $[Pt(CO)_4]^{2+}$, respectively. The apparent weakness in the Pd−CO bonds is reflected in the observed ν(M−C)- and δ(MCO)-stretching and deformation wavenumbers in Tables 8 and S4, when compared to the corresponding fundamentals for $[Pt(CO)_4]^{2+}$. The difference in bond strength between $[Pd(CO)_4]^{2+}$ and $[Pt(CO)_4]^{2+}$ is consistent with differences in thermal stability for $[M(CO)_4][Sb_2F_{11}]_2$, M = Pd, Pt, and the results of the DSC measurements discussed above. The rather weak Pd−CO bonds in $[Pd(CO)_4]^{2+}$ provide a good explanation why there are so few Pd(II) carbonyls known with two or more terminal CO ligands[18−23] in comparison to the more numerous Pt(II) carbonyls of this type.

The observed weakness of the Pd−CO bond, reflected in the trend for the M−C force constants f_{M-C} ($[Pt(CO)_4]^{2+} > [Rh(CO)_4]^+ > [Pd(CO)_4]^{2+}$), is not apparent from the structural data for the isostructural pair $[M(CO)_4][Sb_2F_{11}]_2$, M = Pd, Pt, but is revealed by the vibrational analysis presented above for the tetracarbonyl cations. A detailed bonding discussion for isostructural *cis*-$M(CO)_2(SO_3F)_2$, M = Pd, Pt, has appeared very recently.[73]

Additional results of DFT calculations for the so far unknown square planar d^8 cations $[M(CO)_4]^{n+}$, $M^{n+} = Co^+, Ni^{2+}, Au^{3+}$ and Hg^{4+} are found in the Supporting Information (Tables S4−S6). In the 5d series of isoelectronic D_{4h}-cations $[M(CO)_4]^{n+}$ $\tilde{\nu}$(CO) and f_{CO} gradually increase in the order of $Ir^+ < Pt^{2+} < Au^{3+}$ but then decrease for Hg^{4+}. A similar trend is found for octahedral cations of the type $[M(CO)_6]^{n+}$,[83,98−100] where the strength of the CO bond increases in the order of $Re^+ < Os^{2+} < Ir^{3+} < Pt^{4+}$ but declines for Au^{5+}. It is noteworthy, that the species with a calculated maximum of predicted CO bond strength, square planar $[Au(CO)_4]^{3+}$ and octahedral $[Pt(CO)_6]^{4+}$, have so far remained undetected. The latter cation is not formed in the reductive carbonylation of PtF_6[86] as hoped, but formation of $[Pt(CO)_4]^{2+}$ is observed instead.

(b) ^{13}C NMR Spectroscopy. The spectroscopic characterization of the square planar cations $[Rh(CO)_4]^+$ and $[M(CO)_4]^{2+}$, M = Pd, Pt, in this study is completed by ^{13}C NMR measurements on ^{13}C-enriched samples. For $[Rh(CO)_4]^+$ in HSO_3F at −80 °C, a ^{13}C chemical shift of 173 ppm is noted. Since $[M(CO)_4]^{2+}$, M = Pd, Pt, are converted in HSO_3F to *cis*-$M(CO)_2(SO_3F)_2$, ^{13}C MAS NMR spectra are recorded on solid $[M(CO)_4][Sb_2F_{11}]_2$, M = Pd, Pt. The chemical shifts are 144 and 137 ppm, respectively. The observation that $\tilde{\nu}(CO)_{av}$

increases with increasing nuclear charge, while δ^{13}C decreases within the 4d or 5d series is well established, on the basis of experimental data for $[M(CO)_6]$-species.[48,78]

A similar decrease in ^{13}C chemical shifts vertically down a group is well documented for octahedral metal carbonyl species such as $[M(CO)_6]^{2+}$, M = Fe, Ru, Os,[48,79−82] in group 8, while $\tilde{\nu}(CO)_{av}$ and f_{CO} remain almost constant. The decrease in ^{13}C chemical shifts in a given group appears to be determined by paramagnetic contributions to the chemical shift[96] for both octahedral and square planar carbonyl cations.

Spin coupling constants $^1J(M-^{13}C)$ are only obtainable for $[Rh(CO)_4]^+$ and $[Pt(CO)_4]^{2+}$. For $[Rh(CO)_4]^+$, where ^{103}Rh (100% abundance) with $s = {}^1/_2$, $^1J(^{103}Rh-^{13}C)$ is found to be 61.1 Hz. For $[Pt(CO)_4]^{2+}$ with ^{195}Pt (33.8% abundance) of $s = {}^1/_2$, $^1J(^{195}Pt-^{13}C)$ is found to be 1550 ± 10 Hz in a ^{13}C MAS spectrum and 1576 ± 2 Hz for a solution of $[Pt(CO)_4][Sb_2F_{11}]_2$ in HSO_3F.

Summary and Conclusions

The extensive synthetic, structural, spectroscopic, and computational study of $[M(CO)_4][Sb_2F_{11}]_2$, M = Pd, Pt, described here, establishes the square planar $[M(CO)_4]^{2+}$ cations as an essential part of a series of thermally stable, superelectrophilic metal carbonyl cations. The complete series extends in the 5d-block from groups 12 to 6 and includes linear $[Hg(CO)_2]^{2+}$ [76,77] and $[Au(CO)_2]^+$ ($D_{\infty h}$),[64,67] square planar $[Pt(CO)_4]^{2+}$ (D_{4h}), octahedral $[Ir(CO)_5Cl]^{2+}$ (C_{4v}),[78,83] $[Os(CO)_6]^{2+}$ (O_h),[81,82] and $[Re(CO)_6]^+$ (O_h),[160] and seven-coordinate $[W(CO)_6(FSbF_5)]^+$ (C_{2v}).[84] All can be generated only in superacidic media, [46,47,51−62] and all cations are almost exclusively stabilized by the superacid anion $[Sb_2F_{11}]^-$.[63]

All members in this group are structurally characterized by single-crystal X-ray diffraction. Important members such as $[Au(CO)_2]^+$,[67] $[Pt(CO)_4]^{2+}$, $[Ir(CO)_5Cl]^{2+}$,[83] and $[Os(CO)_6]^{2+}$ [81,82] have also been extensively investigated by a complete vibrational analysis and DFT calculations. With the recently completed molecular structure determinations of *cis*-$M(CO)_2(SO_3F)_2$, M = Pd, Pt,[72,73] *cis*-$Pt(CO)_2Cl_2$,[5] and of the cation $[Rh(CO)_4]^+$ with two different anions, $[1\text{-Et-}CB_{11}F_{11}]^-$ [94] and $[Al_2Cl_7]^-$ [95] the square planar coordination geometry is now very well represented for metal carbonyl compounds.

The detailed structural and spectroscopic characterization of $[M(CO)_4][Sb_2F_{11}]_2$, M = Pd, Pt, completes the extensive characterization of the superelectrophilic metal carbonyl cations for the three principal coordination geometries, linear, square planar, and octahedral. In all superelectrophilic $[M(CO)_n][Sb_2F_{11}]_m$ salts, C- -F interionic contacts are observed and play an important role, while M- -F interactions are either irrelevant or not observed.

Acknowledgment. Financial support by the Natural Sciences and Engineering Research Council of Canada NSERC (operating funds to F.A. and J.T.); Deutsche Forschungsgemeinschaft DFG (operating funds to H.W., PdF scholarship to M.B.); Fonds der Chemischen Industrie (operating funds to H.W.); Schweizerischer Nationalfonds (grant to W.T.); Alexander v. Humboldt Foundation (F. Lynen Fellowship to R.B., Research Prize and re-invitation of F.A.); North Atlantic Treaty Organization NATO (collaborative research grant H.W. and F.A.) is gratefully acknowledged. Dr. G. Balzer (Universität Hannover) is thanked for his help in obtaining ^{13}C NMR spectra. We are indebted to Dr. Brian Patrick (UBC - X-ray crystallography) and Ms. Elizabeth Varty (UBC - Illustrations), who made useful contributions. Dr. Q. Xu and Professor Y. Souma are thanked for preprints of their recent work. Degussa Hüls is thanked for a gift of Pd and Pt metal powder.

Supporting Information Available: Dimensions and design of a Monel-Kel-F reactor used for solution in $HF-SbF_5$; a stereoview of the unit cells of $[M(CO)_4][Sb_2F_{11}]_2$; the molecular structure of $[Pd(CO)_4][Sb_2F_{11}]_2$ showing one formula unit; the $[M(CO)_4]^{2+}$ cations, M = Pd, Pt; selected bifurcated interionic interactions of $[Hg(CO)_2][Sb_2F_{11}]_2$ and $[Pt(CO)_4][Sb_2F_{11}]_2$; the $[Sb_2F_{11}]^-$ anions in $[Pd(CO)_4][Sb_2F_{11}]_2$; interionic contacts [Å] in $[M(CO)_4][Sb_2F_{11}]_2$, M = Pd, Pt; calculated and experimental ^{13}C isotope shifts for the cations $[M(CO)_4]^{n+}$, M = Rh, Pd, Pt, $n = 1, 2$; calculated and experimental vibrational band intensities for $[M(CO)_4]^{n+}$, M = Rh, Ir, Pd, Pt; calculated vibrational wavenumbers (cm^{-1}) and ^{13}CO shifts (cm^{-1}) for square planar (D_{4h}) cations $[M(CO)_4]^{n+}$, M = Co, Ir, Ni, Au, Hg; calculated band intensities for $[Co(CO)_4]^+$, $[Ni(CO)_4]^{2+}$, $[Au(CO)_4]^{3+}$ and $[Hg(CO)_4]^{4+}$; calculated vibrational frequencies (cm^{-1}) at BP86/ECP1 for square planar cations $[M(CO)_4]^{n+}$, M = Co, Rh, Ir (n = 1); Ni, Pd, Pt (n = 2); Au (n = 3) and Hg (n = 4) (PDF). X-ray crystallographic files in CIF format for the complex salts $[Pd(CO)_4][Sb_2F_{11}]_2$ and $[Pt(CO)_4][Sb_2F_{11}]_2$. This material is available free of charge via the Internet at http://pubs.acs.org.

JA002360S